JOURNAL OF GEOPHYSICAL RESEARCH, VOL. ???, XXXX, DOI:10.1029/,

Estimating the summertime tropospheric ozone distribution over North America through assimilation of observations from the Tropospheric Emission Spectrometer

M. Parrington,[1] D. B. A. Jones,[1] K. W. Bowman,[2] L. W. Horowitz,[3] A. M. Thompson,[4] D. W. Tarasick,[5] J. C. Witte,[6,7]

M. Parrington, Department of Physics, University of Toronto, 60 St. George Street, Toronto, Ontario, Canada M5S 1A7 (mark.parrington@utoronto.ca)

[1]Department of Physics, University of Toronto, Toronto, Ontario, Canada.

[2]Jet Propulsion Laboratory, California Institute of Technology, Pasadena, California, USA.

[3]NOAA Geophysical Fluid Dynamics Laboratory, Princeton, New Jersey, USA.

[4]Department of Meteorology, Pennsylvania State University, University Park, Pennsylvania, USA.

[5]Meteorological Services Centre, Environment Canada, Downsview, Ontario, Canada.

[6]Science Systems and Applications Inc., Lanham, Maryland, USA.

[7]Also at NASA Goddard Space Flight Center, Greenbelt, Maryland, USA.

Abstract. We assimilate ozone and CO retrievals from the Tropospheric Emission Spectrometer (TES) for July and August 2006 into the GEOS-Chem and AM2-Chem models. We show that the spatio-temporal sampling of the TES measurements is sufficient to constrain the tropospheric ozone distribution in the models despite their different chemical and transport mechanisms. Assimilation of TES data reduces the mean differences in ozone between the models from almost 8 ppbv to 1.5 ppbv. Differences between the mean model profiles and ozonesonde data over North America are reduced from almost 30% to within 5% for GEOS-Chem, and 40% to within 10% for AM2-Chem, below 200 hPa. The absolute biases are larger in the upper troposphere and lower stratosphere (UT/LS), increasing to 10% and 30% in GEOS-Chem and AM2-Chem, respectively, at 200 hPa. The larger bias in the UT/LS reflects the influence of the spatial sampling of TES, the vertical smoothing of the TES retrievals, and the coarse vertical resolution of the models. The largest discrepancy in ozone between the models is associated with the ozone maximum over the southeastern USA. The assimilation reduces the mean bias between the models from 26 to 16 ppbv in this region. In GEOS-Chem, there is an increase of about 11 ppbv in the upper troposphere, consistent with the increase in ozone obtained by a previous study using GEOS-Chem with an improved estimate of lightning NOx emissions over the USA. Our results show that assimilation of TES observations into models of tro-

pospheric chemistry and transport provides an improved description of free tropospheric ozone.

1. Introduction

Ozone is an important trace gas in the troposphere, playing a significant role in determining the chemical and radiative state of the lower atmosphere. In the lower troposphere ozone is a pollutant contributing to photochemical smog, whereas in the mid-troposphere it is a key precursor of the hydroxyl radical (OH), the primary atmospheric oxidant. In the upper troposphere, strong absorption features in the infrared make ozone a significant greenhouse gas. There have been numerous studies, using chemical transport models (CTMs) and general circulation models (GCMs), that have focussed on quantifying the budget of tropospheric ozone and characterizing its distribution (e.g. *Horowitz et al.* [2003]; *Horowitz* [2006]; *Stevenson et al.* [2006] and references therein). The estimates of the ozone budget from these studies, however, vary significantly, reflecting large uncertainties in the source of ozone from stratosphere-troposphere exchange, loss of ozone due to dry deposition, and in the emissions of ozone precursors [*Wild*, 2007].

Reliable estimates of the budget and distribution of tropospheric ozone are necessary for planning field campaigns using chemical weather forecasts [*Lawrence et al.*, 2003] and for providing insights into future changes in ozone concentrations due to human activity and variations in climate (e.g. *Horowitz* [2006]). For the latter, validation against long-term observations are necessary in giving confidence to such predictions. Studies of long-term trends in tropospheric ozone have been conducted with ozonesonde and surface observations [*Logan*, 1994, 1999; *Tarasick et al.*, 2005; *Oltmans et al.*, 2006] and, while these observations are highly valuable in validating large time-scale model studies, the data have relatively coarse spatial and temporal resolutions compared to those achievable

from satellite observations. Direct measurements of the troposphere, and retrievals of ozone from such measurements, from space-based instruments are challenging due to the low ozone abundances in the troposphere compared to the stratosphere and the presence of clouds.

Until recently, studies of tropospheric ozone using satellite data have relied on empirical techniques combining measurements from different instruments to infer a tropospheric ozone residual column (e.g. *Fishman et al.* [2003]). Information on the vertical distribution of ozone in the troposphere has been retrieved from UV/visible measurements made by the Global Ozone Monitoring Experiment (GOME; for example, *Munro et al.* [1998] and *Tellmann et al.* [2004]). The Tropospheric Emission Spectrometer (TES) [*Beer et al.*, 2001] is the first dedicated infrared instrument from which information about the global and vertical distribution of tropospheric ozone can be retrieved.

Chemical data assimilation provides a powerful tool for optimally combining observations and model data. Various approaches to assimilating observations of trace gases central to tropospheric chemistry have been used in a number of previous studies. Ground-based ozone measurements were assimilated using a 4-Dimensional variational data assimilation (4-Dvar) system by *Elbern and Schmidt* [2001] for studying regional air quality. *Chai et al.* [2007] also used a 4-Dvar system to assimilate surface, aircraft and ozonesonde measurements, while *Clark et al.* [2006] employed a sequential approach to assimilating MOZAIC aircraft data to study cross-tropopause fluxes. A sequential Kalman Filter has been applied for the assimilation of tropospheric ozone columns derived from TOMS [*Lamarque et al.*, 2002] and profiles retrieved from GOME [*Segers et al.*, 2005]. *Pierce et al.* [2007] studied the North American region, illustrating the benefits

of ozone data assimilation for improving the ozone distribution across the upper troposphere and lower stratosphere, employing a statistical digital filter analysis system to assimilate stratospheric ozone profiles and total column ozone into a regional air quality model. Furthermore, *Geer et al.* [2006] presented a comparison of tropospheric analyses from the Assimilation of Envisat data (ASSET) project [*Lahoz et al.*, 2007] which employed different assimilation techniques (Kalman Filter, 3-D and 4-Dvar) in both chemical transport and numerical weather prediction models. These studies highlight the necessity for correctly representing tropospheric chemistry, and high quality observations of the tropospheric ozone distribution.

We present here the first results from the assimilation of vertical profiles of tropospheric ozone from the TES instrument in global models of tropospheric chemistry and transport. Ozone is a key species in the chemistry of the tropopshere and assimilation of global observations of ozone may provide valuable information on the processes controlling its distribution. A challenge in assimilating tropospheric ozone observations is that the distribution of tropospheric ozone is heterogeneous, reflecting the influences of transport and local photochemical sources and sinks. Also, the lifetime of tropospheric ozone is highly variable, increasing from days in the lower troposphere to months in the upper troposphere. Reliably constraining the ozone distribution in a chemical data assimilation context, therefore, requires observations with sufficient spatial and temporal resolution to capture the heterogeneity in the ozone distribution and to overcome the loss of information in the assimilation associated with the short lifetime of ozone in the lower and middle troposphere. We examine the potential of TES observations of ozone to provide a consistent description of tropospheric ozone when they are assimilated into two different

models of tropospheric chemistry and transport (GEOS-Chem and AM2-Chem), with different chemical and transport schemes. AM2-Chem is a general circulation model (GCM) designed for chemistry-climate studies. For computational expedience it has a simplified representation of the oxidation of non-methane hydrocarbon (NMHC) chemistry. GEOS-Chem is a global chemistry transport model (CTM) with a complete treatment of the NMHC chemistry. Our objective here is to demonstrate the potential of assimilation of data from TES for constraining the distribution of ozone in these models, which ultimately will enable us to better identify errors in the chemical processes that control ozone in the models.

2. Tropospheric Emission Spectrometer Ozone Profile Retrievals

The Troposphere Emission Spectrometer (TES) [*Beer et al.*, 2001] is a high-resolution imaging infrared Fourier-transform spectrometer, launched aboard the NASA EOS Aura satellite on July 14, 2004. The Aura satellite is in a polar Sun-synchronous orbit with a repeat cycle of 16 days. The instrument utilizes a nadir-viewing geometry and an instrument field-of-view at the surface of 8 km $\times$ 5 km to observe spectral radiances in the range 650-3050 cm^{-1} at an apodized spectral resolution of 0.1 cm^{-1}. It operates in a global survey mode, in which the observations are spaced about 220 km along the orbit track, and in a step-and-stare mode, in which the observations are spaced every 30 km long the orbit track. Geophysical parameters are retrieved from the radiances based on a Bayesian framework that solves a constrained nonlinear least squares problem [*Bowman et al.*, 2006]. The retrieved ozone profile $\hat{\mathbf{x}}$ is an estimate of the atmospheric state which can be expressed as

$$\hat{\mathbf{x}} = \mathbf{x}^{apriori} + \mathbf{A}(\mathbf{x} - \mathbf{x}^{apriori}) + \mathbf{Gn} \tag{1}$$

assuming that the estimate is spectrally linear with the true state [*Rodgers*, 2000; *Bowman et al.*, 2002]. Here $\mathbf{x}^{apriori}$ is the *a priori* profile applied in the retrieval, $\mathbf{x}$ is the true atmospheric profile, $\mathbf{A}$ is the averaging kernel matrix, $\mathbf{G}$ is the gain matrix and $\mathbf{n}$ is a vector whose elements contain the spectral measurement noise (the covariance of this spectral measurement error is $\mathbf{S}_n = E[\mathbf{nn}^T]$). For the retrieval of ozone and other trace gases, $\hat{\mathbf{x}}$ and $\mathbf{x}^{apriori}$ are expressed in terms of the natural logarithm of the volume mixing ratio (VMR). Vertical profiles are retrieved on a vertical grid of 67 levels with a discretization of approximately 1km per level [*Clough et al.*, 2006] although the vertical resolution of the retrieval is much coarser.

The averaging kernels give the sensitivity of the retrieved state to the true state of the atmosphere. The trace of the averaging kernel matrix gives a measure of the number of independent pieces of information available in the measurements, more commonly referred to as the degrees of freedom for signal (DOFS) [*Rodgers*, 2000]. Figure shows TES ozone and CO retrieval characteristics for 15 August 2006. On average, for ozone there are between three and four DOFS for the full retrieved profile (shown by the black crosses in Figure a) and less than 1.5 DOFS for the tropospheric part of the profile north of 20° S. Discontinuities in the DOFS at different latitudes are due to changes in the constraint matrix used in the retrieval [*Kulawik et al.*, 2006; *Osterman et al.*, 2007]. The TES CO retrievals are sensitive primarily to CO in the troposphere, as shown in Figure c, with between 1.0 and 1.5 DOFS for the tropospheric profile. The stratospheric retrieval adds approximately 0.5 DOFS to the tropospheric profile retrieved for CO.

Averaging kernels for the troposphere and lower stratosphere for profiles of ozone and CO retrieved over the southeastern USA at 30° N and 87° W on 15 August 2006 are shown in Figures b and d respectively. Of the total 3.92 DOFS for the retrieved profile of ozone, 1.15 comes from the troposphere indicating a reasonable level of sensitivity in the troposphere, particularly between 1000 and 500 hPa as shown by the averaging kernels coloured red. In the mid-troposphere and upper troposphere/lower stratosphere, the information is spread over a wider vertical range, illustrating the coarse vertical resolution. For the CO retrieval, the troposphere contributes 1.12 to the total of 1.58 DOFS. The CO retrieval shows peak sensitivity in the lower troposphere, between 1000 and 500 hPa similar to the ozone profile, while the peak sensitivities for the mid-troposphere and upper troposphere/lower stratosphere are located mainly in the upper troposphere with less spreading of information across the tropopause compared to the ozone retrieval.

Tropospheric ozone profile retrievals from TES have previously been used to study ozone over the tropical Atlantic during the northern African biomass burning season [*Jourdain et al.*, 2007]. *Worden et al.* [2007] reported that V001 of the TES ozone retrieval are biased high, compared to ozonesonde profiles, in the upper troposphere, while *Nasser et al.* [in press] reported that V002 of the TES ozone retrieval are biased high compared to ozonesondes by 2.9 - 10.6 ppbv in the upper troposphere and 0.7 - 9.2 ppbv in the lower troposphere. It is postulated that these systematic biases could be due to known problems with the temperature profiles, retrieved jointly with ozone, which are expected to be reduced in V003 of the retrieval. TES retrievals of CO have been compared with profile retrievals of CO from the Measurements of Pollution in The Troposphere (MOPITT) instrument [*Luo et al.*, 2007a] and have been validated with *in situ* observations from

aircraft [*Luo et al.*, 2007b]. *Luo et al.* [2007b] showed that the mean difference between column abundances of CO from TES and MOPITT were less than 5%. In this paper, profiles of ozone and CO retrieved from the TES observations are assimilated into the models described in the next section. These data are version V002.R9.3 of the TES level 2 global survey products. Only retrievals between ±80° latitude are used in the analysis, and prior to performing the assimilation, the data are filtered based on the mean and root mean square of the radiance residual and on the cloud top pressure of each profile, following the TES L2 Data User's Guide [*TES Science Team*, 2006].

3. The GEOS-Chem and AM2-Chem Models

3.1. AM2-Chem

The GFDL Atmospheric Model 2 (AM2) general circulation model is described in detail by *GFDL GAMDT* [2003]. The version of the model employed here has a horizontal resolution of 2 degrees latitude by 2.5 degrees longitude with 24 vertical levels from the surface to approximately 3 hPa. There are nine levels in the lowest 1.5 km above the surface, whereas there are five levels in the stratosphere. The vertical resolution in the upper troposphere is about 2 km. This version of the AM2 has online tropospheric gas-phase and aerosol chemistry (and is referred to as AM2-Chem). The emissions, chemistry (ozone-NO_x-CO-hydrocarbon, sulphate and carbonaceous aerosols) and deposition rates in the model are based on the MOZART-2 chemical transport model [*Horowitz et al.*, 2003; *Tie et al.*, 2005]. It has approximately 41 chemical species and 100 chemical reactions. The model chemistry is simplified with a reduced isoprene chemistry designed to approximate the production of ozone and PAN from isoprene. Biogenic emissions of isoprene and acetone are 410 TgC and 37 TgC per year, as described in *Horowitz et al.*

[2003], but higher order NMHCs are not included. The production of NO_x from lightning is calculated for convective clouds by examining the cloud base temperature and then estimating the flash frequency and resulting NO emissions, based on *Price et al.* [1997], with the vertical distribution based on *Pickering et al.* [1998]. Methane concentrations are fixed in the simulations presented here at 1629 ppbv. The ozone distribution in the stratosphere (i.e. above 100 hPa) is represented by a HALOE climatology [*Randel and Wu*, 1999], whilst stratospheric distributions of CO, NO_x, HNO_3, N_2O and N_2O_5 are relaxed to climatological values from the Study of Transport and chemical Reactions in the Stratosphere (STARS) model [*Brasseur et al.*, 1997]. In addition, the model dynamics, for the simulations presented in this paper, are constrained by nudging to re-analyses from NCEP. This ensures that the simulated synoptic features in the GCM are consistent with observations.

3.2. GEOS-Chem

The GEOS-Chem chemical transport model is a global 3-D model driven by assimilated meteorological observations from the NASA Goddard Earth Observing System (GEOS-4) from the Global Modeling and Assimilation Office (GMAO). The meteorological fields have a horizontal resolution of 1 degree latitude by 1.25 degrees longitude with 55 levels in the vertical, and a temporal resolution of 6 hours (3 hours for surface fields). The first generation of the model, along with a comparison of model results with observations, was presented in *Bey et al.* [2001]. Recent updates and applications of the model have been described in a range of studies (e.g. *Fiore et al.* [2003]; *Hudman et al.* [2004]; *Liang et al.* [2007]). The model includes a complete description of tropospheric O_3-NO_x-hydrocarbon chemistry, including sulphate aerosols, black carbon, organic carbon, sea salt, and dust.

Anthropogenic emissions in the model are from the Global Emissions Inventory Activity (GEIA) [*Benkovitz et al.*, 1996], as described in *Duncan et al.* [2007]. For the United States these emissions are replaced with those from the Environmental Protection Agency (EPA) National Emission Inventory 1999 (NEI99) [*Hudman et al.*, 2007]. Biomass burning emissions are based on *Duncan et al.* [2003] while biofuel emissions are from *Yevich and Logan* [2003]. Biogenic emissions of isoprene and acetone are 392 TgC and 40 TgC per year respectively which are comparable with those in AM2-Chem. The model also includes biogenic emissions of 104 TgC per year for monoterpenes and 11 TgC per year for ≥C3 alkenes. Methane concentrations are specified as 1706, 1710, 1768 and 1823 ppbv, imposed for latitude bands between 90-30° S, 30° S-0°, 0°-30° N, and 30-90° N. The lightning source of NO_x in GEOS-Chem is estimated, following *Price and Rind* [1992], based on deep convective cloud top heights, which are provided with the GMAO meteorological fields. The vertical distribution of the source is imposed according to *Pickering et al.* [1998]. In this paper, we are using v7-02-04 of GEOS-Chem with a horizontal resolution of 2 degrees latitude by 2.5 degrees longitude. The ozone in the stratosphere is represented by a linearized ozone (Linoz) parameterization [*McLinden et al.*, 2000].

4. Data Assimilation Methodology

Profiles of ozone and carbon monoxide from TES are assimilated into the AM2-Chem and GEOS-Chem models in a sequential manner using a sub-optimal Kalman Filter (following *Khattatov et al.* [2000]). For each observed profile, we calculate an expected analysis profile $\hat{\mathbf{x}}^a$ as given by the expression

$$\hat{\mathbf{x}}^a = \mathbf{x}^f + \mathbf{K}(\hat{\mathbf{x}}^{obs} - \mathbf{H}\mathbf{x}^f) \tag{2}$$

where $\mathbf{K}$ is the Kalman gain matrix, $\mathbf{H}$ is the observation operator, $\mathbf{x}^f$ is the model (or forecast) profile, and $\hat{\mathbf{x}}^{obs}$ is the retrieved TES profile (i.e. $\hat{\mathbf{x}}$ in equation 1). As the TES trace gas profiles are retrieved as the natural logarithm of VMR, the assimilation is performed with respect to the logarithm of the VMR. Because of the vertical smoothing of the true state by the TES retrievals, the analysis in equation 2 is performed in the measurement space of TES. The observation operator $\mathbf{H}$ transforms the higher resolution model profile by interpolating the profile to the TES vertical grid and accounting for the TES *a priori* profile $\mathbf{x}^{apriori}$ and the vertical smoothing of the retrievals as reflected by the averaging kernels ($\mathbf{A}$). The observation operator is given by

$$\mathbf{H}\mathbf{x}^f = \mathbf{x}^{apriori} + \mathbf{A}(\mathbf{x}^f - \mathbf{x}^{apriori}) \tag{3}$$

Note that, when equation 3 is substituted back into equation 2 to calculate the analysis increment, with the TES retrieval defined as in equation 1, the influence of the *a priori* is removed from the retrieved profile $\hat{\mathbf{x}}^{obs}$ [*Jones et al.*, 2003]. In the AM2-Chem model, which has a top vertical level at 10 hPa, the interpolated profile in the stratosphere is replaced by the TES *a priori* profile.

The Kalman gain matrix is defined as:

$$\mathbf{K} = \mathbf{P}^f\mathbf{H}^T(\mathbf{H}\mathbf{P}^f\mathbf{H}^T + \mathbf{R})^{-1} \tag{4}$$

where $\mathbf{P}^f$ is the error covariance matrix of the forecast profile and $\mathbf{R}$ is the observation error covariance matrix provided with the TES retrieval. The analysis error covariance matrix is calculated as

$$\mathbf{P}^a = (\mathbf{I} - \mathbf{K}\mathbf{H})\mathbf{P}^f \tag{5}$$

where $\mathbf{I}$ is the identity matrix. In the experiments presented here, the analysis error variance is transported as a passive tracer following *Ménard et al.* [2000] for GEOS-Chem, while AM2-Chem has a fixed variance. Retrieved ozone and CO profiles from TES are assimilated for 1 July through to 31 August 2006 with a 6-hour analysis cycle (i.e. the TES data are ingested into the model every 6 hours) and with an assumed initial forecast error of 50% of the initial forecast field which we assume also captures the representativeness error. It is important to note that the current assimilation set-up is sub-optimal in that it neglects horizontal correlations in the forecast error covariance matrix (i.e. $\mathbf{P}^f$ is assumed to be block diagonal). Vertical correlations due to the smoothing influence of the TES retrievals are accounted for in the forecast error covariance matrix through the influence of the averaging kernels in the observation operator $\mathbf{H}$ in equation 3, and which operates on $\mathbf{P}^f$ in equation 4.

The TES profile retrievals are ingested along the orbit track, within each assimilation window, after filtering as described in Section 2. We assimilate the same number of observations of CO and ozone in both models. Although we assimilate the CO and ozone data simultaneously, we treat them independently and do not account any CO-ozone covariance in the forecast error covariance matrix. The CO and ozone assimilation, however, are coupled chemically though their impact on the tropospheric chemistry. In both models the analysis increments for CO and ozone in equation 2 are set to zero above 100 hPa in order to constrain only the trace gas profiles in the troposphere.

5. Results

5.1. North American Ozone Distribution

Monthly averaged ozone concentrations over North America for August 2006, simulated in the AM2-Chem and GEOS-Chem models with and without assimilation, are shown in Figure . Without assimilation of the TES data there are significant differences in the ozone distribution between the two models. In particular, there is substantially more ozone in the GEOS-Chem model over the eastern United States of America. These discrepancies may be attributed to the differences in the chemical mechanisms between the two models. AM2-Chem has a simplified representation of NMHC chemistry to GEOS-Chem and, as discussed below, has a much lower source of lightning NO_x compared to GEOS-Chem. There are large differences over the eastern Pacific, where there is much more ozone in the GEOS-Chem model than in AM2-Chem. Assimilation of the TES data results in an increase in the monthly mean ozone abundance over North America in both models, with larger increases in AM2-Chem than in GEOS-Chem. In general, the ozone increases in AM2-Chem are generally between 15-60% compared to 0-30% in GEOS-Chem. Sensitivity tests conducted using a fixed forecast error variance in GEOS-Chem produced only small absolute differences of less than 3% in the ozone analysis.

As a result of the assimilation, the large-scale structures in the ozone distribution are more consistent between the models. This is especially noticeable over the eastern Pacific and western Atlantic. The consistency of the assimilated ozone fields is further illustrated in the top two panels of Figure , which shows scatterplots of the simulated ozone distribution in AM2-Chem versus GEOS-Chem at 5 km altitude across the domain shown in Figure (i.e. 150 to 50° W and 15 to 65° N) for each day in August 2006. The mean

difference between the simulated ozone distributions in the middle troposphere over North America for August, in GEOS-Chem relative to AM2-Chem, is reduced from 7.6 ppbv to -1.5 ppbv following assimilation of the TES data. In addition, the slope of the scatter plot is increased from 0.4 to 0.6. Although the global mean difference between the models increases from 1.9 ppbv to -2.7 ppbv as a result of the assimilation (not shown). This is attributable to AM2-Chem having more ozone in the southern hemisphere than GEOS-Chem and the assimilation providing greater constraints on ozone in the northern hemisphere troposphere, due to the higher thermal contrast between the surface and atmosphere in summer and, therefore, more DOFS in the retrievals in the norther hemisphere (Figure).

Figure shows the same results as Figure for daily averaged ozone concentrations for 15 August 2006. The scatter plot for this data is shown in the lower two panels of Figure . For this date the results are very similar to those for the monthly mean with considerable differences in the ozone distributions between the two models which are reduced following the assimilation of the TES data. In both models the synoptic features are enhanced in the assimilation. In this case ozone generally increases by between 20-60% in AM2-Chem (and up to 100% in some regions, such as south of 30° N) compared to between 0-40% in GEOS-Chem. Similarly, the mean difference between the models is reduced from 7.2 ppbv to -1.8 ppbv following the assimilation, with the slope of the scatter plot increased from 0.5 to 0.7. It is important to note that the correlation coefficients for the scatter plots (Figure) do not change significantly following the TES assimilation, increasing slightly from 0.54 to 0.56 for the whole month and decreasing from 0.6 to 0.57 for 15 August. This is because, although the magnitude of the ozone abundance can be retrieved from

TES, the TES data do not provide sufficient spatial coverage to adequately sample the fine scale spatial structure in the tracer distribution.

Recently, there has been much interest in the distribution of tropospheric ozone over eastern North America [*Li et al.*, 2005; *Cooper et al.*, 2006, 2007; *Hudman et al.*, 2007]. During boreal summer ozone concentrations in this region are enhanced due to the interaction of different processes. *Thompson et al.* [2007a, b] found during the summer of 2004 that convective transport of ozone and its precursors along with free-tropospheric pollution, and cross-tropopause transport from the stratosphere contribute approximately 25% each to the tropospheric column budget over North America, with the remainder from aged background ozone. We find that there are considerable differences between the models over this region which the assimilation of TES data reduces although it does not completely account for all of the difference; the mean bias over the southeastern USA (100-80° W and 30-40° N) in August is reduced from 26 ppbv to 16 ppbv (not shown).

A prominent feature in the North American distribution of ozone is the summertime enhancement of ozone over the background over the southern USA. Recent studies by *Cooper et al.* [2006, 2007] and *Hudman et al.* [2007] suggest that NO_x emissions from lightning may play an important role in the formation of this summertime ozone maximum. Figure shows the monthly averaged lightning NO_x emissions at 5 km altitude for August 2006 in AM2-Chem and GEOS-Chem in units of $cm^{-3}s^{-1}$. The total emissions of NO_x from lightning over this region for August 2006 are 0.012 TgN in AM2-Chem and 0.064 TgN in GEOS-Chem. These lightning emissions are comparable to the source of 0.068 TgN reported by *Hudman et al.* [2007] for their GEOS-Chem simulation for 1 July to 15 August 2004, which was a factor of 4 too low than the estimate of 0.27 TgN that they

calculated based on lightning flash rates from the National Lightning Detection Network (NLDN). *Hudman et al.* [2007] found the higher NO_x emissions from lightning provided an improved simulation of aircraft observations during the International Consortium for Atmospheric Research on Transport and Transformation (ICARTT) campaign in summer 2004. As discussed in section 5.4, our assimilation of the TES CO data implies that it is unlikely that the underestimate of ozone in the GEOS-Chem model is due to an underestimate of the hydrocarbon precursors. Furthermore, the assimilation produces a mean increase in ozone of about 11 ppbv, averaged over 5 to 10 km and 30-40° N and 100-80° W. This is consistent with the 10 ppbv increase in ozone obtained by *Hudman et al.* [2007] in the upper troposphere with their improved NO_x emissions from lightning. It is also in agreement with the 11-13 ppbv of ozone produced by lightning NO_x estimated by *Cooper et al.* [2006]. Our results suggest that higher NOx emissions from lightning, as suggested by *Hudman et al.* [2007], may indeed be required to reconcile the a priori discrepancy between the simulated ozone in GEOS-Chem and the ozone observations from TES over southeastern North America.

Differences in the global source of NO_x from lightning will contribute to differences in the background ozone abundances over North America in the two models. The global emissions of NO_x from lightning in AM2-Chem is about 2 $TgNyear^{-1}$, whereas in GEOS-Chem it is 4.7 $TgNyear^{-1}$. Based on constraints imposed on GEOS-Chem from space-based observations of lightning flash counts, *Sauvage et al.* [2007] recommended a global lightning source of 6 $TgNyear^{-1}$. They found that this improved the ozone simulation in the model in the tropical upper troposphere by between 10 and 45%, but the improvements were highly sensitive to the spatial distribution of the lightning NO_x emissions.

5.2. Vertical Distribution of Ozone

The vertical distribution of ozone throughout the troposphere reflects a combination of *in situ* photochemical production of ozone, convective transport of ozone and its precursors from the boundary layer, and cross-tropopause transport of ozone from the stratosphere. The interplay of these factors is most apparent over the eastern USA, as shown in Figures and . The panels in Figures and show the ozone and NO_x vertical distribution in the models at 75° W as a function of latitude and at 40° N as a function of longitude respectively. In both models there are large abundances of NO_x in the boundary layer and lower troposphere over continental North America. This contributes to the ozone abundance in the middle and upper troposphere due to strong convection over the southeastern United States at this time of year, which lifts ozone precursors up from the boundary layer.

There is a large discrepancy between the two models in the abundance of NO_x in the the upper troposphere, due to the differences in the lightning NO_x emissions. In the GEOS-Chem model this secondary maximum in the NO_x concentrations is centered around 10 km at 35° N and 85° W, while in the AM2-Chem model it is absent. This contributes significantly to the differences in the ozone distribution between the models, particularly between 30 and 40° N. As shown in Figure , assimilation of the TES ozone data does reduce the discrepancy in ozone between the two models. *Cooper et al.* [2007], using ozonesonde data, locate the centre of the North American summertime ozone maximum approximately over Alabama (around 35° N and 85° W), which agrees well with the assimilated model results. For comparison, we show in Figure the vertical distribution of the modeled ozone obtained from GEOS-Chem without NO_x emissions from lightning. Without NO_x

from lightning the ozone maximum in the upper troposphere over the southeastern United States is significantly diminished.

It should be noted that in addition to increasing the ozone abundance in the upper troposphere in AM2-Chem, the assimilation also lowers the position of the modeled ozone tropopause. This smoothing of the vertical gradient in ozone across the tropopause is due to the course vertical resolution of the TES retrievals and the coarse vertical resolution in the upper troposphere and lower stratosphere (UT/LS) of the version of the AM2-Chem model used here. In contrast, in the GEOS-Chem model, which has greater vertical resolution in the UT/LS (and is more comparable to the TES retrieval grid), there is less of a change in position of the ozone tropopause after assimilation of the TES data. The lower position of the tropopause in AM2-Chem (both before and after assimilation) leads to higher values of stratospheric NO_x around 15 km, compared to GEOS-Chem, due to the STARS climatology described previously. These NO_x values are distinct from those produced from lightning emissions and are not expected to contribute to ozone production in the upper troposphere.

At higher latitudes (poleward of 45° to 50° N), the differences in the vertical distribution of ozone between the models are much less. The ozone abundance in the middle and upper troposphere at these latitudes reflects the filament stretching across Central North America in Figure , associated with an intrusion of air from the stratosphere, and which assimilation of TES data enhances in both models. The filament originates in the eastern Pacific and is due to downward transport of ozone from the stratosphere off the coast of the western United States (Figure). In both models this downward transport of ozone is enhanced by assimilation. However, in AM2-Chem, the fold in the tropopause, centered

around 120° W, is broadened, compared to GEOS-Chem, as a result of the assimilation, potentially reflecting the coarser vertical resolution of AM2-Chem and the smoothing influence of the TES retrievals. *Thompson et al.* [2007a, b] report that in the middle to upper troposphere, especially over northeastern North America, layers of ozone from the different sources mentioned previously interleave with one another, and, despite the coarse vertical resolution, TES may have some sensitivity to these features.

5.3. Comparison to Ozonesonde Data

To verify the changes introduced by the assimilation to the modelled ozone fields, we compared the assimilated fields to ozonesonde profiles measured by the INTEX Ozonesonde Network Study 2006 (IONS-06) (*http://croc.gsfc.nasa.gov/intexb/ions06.html*, *Thompson et al.* [2007a, b]). During August 2006, 423 ozonesonde profiles were launched from 23 stations across North America as summarized in Table 1. Figure shows a comparison between individual AM2-Chem and GEOS-Chem ozone profiles and ozonesonde profiles measured at a number of different locations across North America on 15 August 2006. In most cases, the TES assimilation leads to an increase in ozone in both models throughout the atmosphere, which improves the model profile relative to the ozonesonde profiles. In some cases, particularly over the eastern North America (Beltsville, Huntsville, Narragansett and Walsingham), the surface emissions in the two models lead to an overestimate in the ozone abundance in the lower troposphere which the assimilation cannot correct due to limited sensitivity of the TES measurements to ozone in the boundary layer. The comparison in the upper troposphere shows, in general, that the assimilated GEOS-Chem profiles are in better agreement with the ozonesonde data, whereas the assimilated AM2-

Chem profile typically overestimate the ozone abundance (as illustrated, for example, in the profiles from Beltsville and Walsingham).

The mean difference between the models and the IONS-06 data during August 2006 are shown in Figure . Without assimilation the mean difference between the AM2-Chem profiles and the sonde data is large, up to almost -40% in the mid-troposphere. Assimilation of TES data reduces this considerably, down to within 10% in the mid-troposphere. In the upper troposphere in AM2-Chem, the model profile is greater than the ozonesonde profile by almost 20% which is further increased following the assimilation, to more than 50%, reflecting the coarse vertical resolution in the model over that part of the atmosphere and issues with mapping the AM2-Chem model profiles to the TES retrieval grid (which has a relatively finer vertical resolution) in the assimilation. The mean differences between the GEOS-Chem profiles and the sonde data are smaller than in AM2-Chem, of order 15-20% in the lower to mid-troposphere and up to 30% at 200 hPa. Following assimilation of TES data, the mean differences between the GEOS-Chem and ozonesonde profiles are greatly reduced, to less than 5% throughout the atmosphere up to about 200 hPa where it increases up to approximately 10%. This is not as great as the change in the AM2-Chem profiles in the upper troposphere, and is well within the variability of the ozonesonde profiles. This difference in the response of the models to the assimilation in the upper troposphere and lower stratosphere reflects the higher vertical resolution of GEOS-Chem in this region of the atmosphere.

The mean atmospheric state is mostly determined by large scale processes, such as inter-continental transport, that have sufficient spatio-temporal scales to be well sampled by TES, giving rise to the improvements in the mean model profiles shown in Figure .

As shown in Figure , individual ozonesonde profiles exhibit detailed vertical structure which is not captured by the models before or after the assimilation of TES data. This fine vertical structure is due to short spatio-temporal scale processes which the models are unable to resolve, and TES does not sample the atmosphere with sufficient density to have an impact through the assimilation. Therefore, we do not expect the TES assimilation to improve the model variability relative to the ozonesondes. The standard deviation of the mean profiles is shown in Figure (c) and (f). Without the TES assimilation, the standard deviation of the two model profiles is less than that of the ozonesonde profiles by 20 to 50 ppbv throughout the troposphere. Below approximately 300 hPa, the TES assimilation has little impact on the standard deviation, reflecting the limitations in representing the small scale atmospheric processes. Above 300 hPa, the assimilation improves the standard deviation relative to the ozonesondes, reflecting the increase in ozone lifetime with increasing altitude which in turn subjects the ozone profile to larger scale processes which are captured by TES.

5.4. Impact of the CO Assimilation on Ozone

Atmospheric CO is a byproduct of incomplete combustion and is produced from the oxidation of atmospheric hydrocarbons. It is a precursor of tropospheric ozone and because of its long lifetime it is a useful proxy for the long-range transport of other ozone precursors from combustion and biogenic sources. To isolate the contribution of the assimilation of CO data to the change in troposphere ozone shown in the previous sections, we examine here the results obtained when only the TES CO data are assimilated.

The modeled CO distribution and the changes in CO produced by the assimilation are shown in Figure . In the AM2-Chem model the assimilation increases the concentration

of CO throughout the free troposphere across North America, with increases of up to 20-25% in the middle troposphere, poleward of 45° N. Over the southern US, in the region of the ozone maximum, the changes are approximately 10%. In the GEOS-Chem model the assimilation produces increases in CO of about 5% in the high latitudes, poleward of 45° N. Over the southern United States, however, the assimilation results in a 5-10% reduction in the CO abundance in GEOS-Chem. The different response in the models to the CO assimilation is likely due to the fact that AM2-Chem explicitly accounts for only isoprene and acetone biogenic emissions, whereas GEOS-Chem includes the higher NMHCs. Nevertheless, the changes in CO due to the assimilation are much smaller than the changes in ozone presented earlier.

The changes in the tropospheric ozone abundances produced by the CO assimilation are shown in Figure . As with CO, the ozone concentrations in AM2-Chem increase across North America, with the largest increases of 6-8% at higher latitudes. Over the southern United States the increases were only 2-6%. In comparison, the increase in ozone in AM2-Chem were between 25-50% when both CO and ozone observations were assimilated. In GEOS-Chem, which has a more complete treatment of the NMHC oxidation chemistry, the absolute CO-induced changes in ozone are small, less than 1%. Over the southern United States the ozone concentrations in GEOS-Chem also decrease by less than 1% as a result of the reduced CO in this region in the assimilation. *Li et al.* [2005] showed that biogenic emissions represent the dominant contribution to CO over southeastern North America in summer. The reduced CO in the GEOS-Chem assimilation suggests that it is unlikely that the underestimate of ozone in the model in this region, relative to TES, is due to an underestimate of the hydrocarbon precursors of ozone in GEOS-Chem. It

implies that the underestimate of NO_x emissions from lightning, as discussed above, is the likely source of the ozone discrepancy.

6. Conclusions

We have presented a framework for, and the first results of, the assimilation of tropospheric ozone profiles retrieved from measurements made by the TES instrument. We used a sequential sub-optimal Kalman filter to assimilate observations of CO and ozone into the AM2-Chem and GEOS-Chem models for July - August 2006. Assimilation of the TES data improves significantly the consistency of the ozone distribution between the two models, despite differences in the chemical and transport schemes of the models. For example, the version of AM2-Chem used here has a more simplified representation of non-methane hydrocarbon chemistry then GEOS-Chem, and has a global source of NO_x from lightning of 2 TgN per year compared to 4.7 TgN per year in GEOS-Chem. Assimilation of TES data significantly increases the ozone abundances in both models. Over North America the assimilation reduces the absolute mean difference in ozone in the middle troposphere between the two models from about 8 ppbv to about 1.5 ppbv. This reduction in the mean ozone difference between the two models demonstrates that the TES data have sufficient information for constraining the ozone distribution in the models.

The major discrepancy in the ozone simulation over North America between the two models is in the upper troposphere over the southeastern United States, where the GEOS-Chem model produces significantly more ozone than the AM2-Chem model. The higher abundances of ozone in GEOS-Chem are associated with a secondary maximum in the abundance of NO_x in the upper troposphere, due to emissions of NO_x from lightning.

In AM2-Chem NO_x emissions from lightning over North America are about a factor of five smaller than in GEOS-Chem and the secondary maximum in NO_x in the upper troposphere over the southeastern United States is absent. Assimilation of TES data enhances ozone abundances in this region in both models. In GEOS-Chem, ozone increases by about 11 ppbv in the upper troposphere, which is consistent with the increase in upper tropospheric ozone obtained by *Hudman et al.* [2007] using GEOS-Chem with an improved lightning NO_x source. In AM2-Chem the assimilation increases the ozone abundance and reduces the gradient in ozone across the tropopause in the model. In contrast, the change in the gradient in ozone across the tropopause is much less in GEOS-Chem. The change in ozone across the tropopause in AM2-Chem is due to the smoothing influence of the TES retrievals and the coarse vertical of the version of AM2-Chem used in the analysis. Although the assimilation tries to compensate for the bias in ozone in the upper troposphere over the southeastern United States in AM2-Chem, a large residual bias in the model clearly indicates the critical need for correctly representing emissions in the chemistry.

Comparison of the assimilated ozone fields with ozonesonde measurements from the IONS-06 campaign in August 2006 show that both models, following assimilation are in better agreement with the sonde data and provide a more accurate description of the vertical distribution of ozone in the troposphere. Over North America the GEOS-Chem model has a mean bias with respect to the ozonesonde profiles reaching a maximum of -30% at 200 hPa, while the maximum mean bias in AM2-Chem is almost -40% around 500 hPa. Following assimilation, the absolute bias in GEOS-Chem is reduced to less than 5% between 800-200 hPa, whereas in AM2-Chem the absolute bias in the assimilated ozone

fields is less than 10% between 800-300 hPa. We found that the assimilation increased significantly the bias in the AM2-Chem ozone fields, relative to the sonde data, in the upper troposphere, between 300-100 hPa. As discussed above, this is due to the coarse vertical resolution of the version of the AM2-Chem model used here. Vertical profiles retrieved from a nadir infrared viewing satellite instrument such as TES will have a coarse vertical resolution, with averaging kernels reflecting the smoothing of information over a large vertical range. When this is combined with a model with coarse vertical resolution, the assimilation can lead to an overestimate of the ozone in the upper troposphere. In GEOS-Chem this is less of an issue than in AM2-Chem as its vertical resolution is more comparable to that of TES retrieval grid. This clearly illustrates the necessity for higher resolution data and models in the upper troposphere and lower stratosphere to accurately reproduce the ozone distribution in this region of the atmosphere. Indeed, the resolution issues related to AM2-Chem are expected to be resolved with forthcoming improvements to the model in AM3, which will have 48 levels with a vertical resolution of 1 km in the UT/LS.

The dramatic improvement obtained in the comparisons between the models and the ozonesonde data after assimilation demonstrates that TES does indeed provide valuable information on the distribution of tropospheric ozone and that assimilation of this information into GCMs or CTMs can produce a significantly improved description of ozone abundances in the free troposphere in these models. This will be valuable for a range of applications, such as chemical weather forecasting, estimating the contribution from tropospheric ozone to the radiative forcing of the climate system, and obtaining a better understanding of the underlying chemical processes controlling tropospheric ozone.

Acknowledgments. This work was supported by funding from the Canadian Foundation for Climate and Atmospheric Sciences (CFCAS) and the Natural Sciences and Engineering Research Council (NSERC). The GEOS-Chem model is maintained at Harvard University with support from the the NASA Atmospheric Chemistry Modeling and Analysis Program.

References

Beer, R., T. A. Glavich, and D. M. Rider (2001), Tropospheric emission spectrometer for the Earth Observing System's Aura satellite, *Applied Optics*, *40*(15), 2,356–2,367.

Benkovitz, C. M., M. T. Scholtz, J. Pacyna, L. Tarrasón, J. Dignon, E. C. Voldner, P. A. Spiro, J. A. Logan, and T. E. Graedel (1996), Global gridded inventories of anthropogenic emissions of sulfur and nitrogen, *Journal of Geophysical Research*, *101*(D22), 29,239–29,253.

Bey, I., et al. (2001), Global modeling of tropospheric chemistry with assimilated meteorology: Model description and evaluation, *Journal of Geophysical Research*, *106*(D19), 23,073–23,095.

Bowman, K. W., J. Worden, T. Steck, H. M. Worden, S. Clough, and C. D. Rodgers (2002), Capturing time and vertical variability of tropospheric ozone: A study using TES nadir retrievals, *Journal of Geophysical Research*, *D23*(4723), *doi:10.1029/2002JD002150*.

Bowman, K. W., et al. (2006), Tropospheric emission spectrometer: Retrieval method and error analysis, *IEEE Transactions on Geoscience and Remote Sensing*, *44*(5), 1,297–1,307.

Brasseur, G. P., X. Tie, P. J. Rasch, and F. Lefèvre (1997), A three-dimensional simulation of the Antarctic ozone hole: Impact of anthropogenic chlorine on the lower stratosphere and upper troposphere, *Journal of Geophysical Research*, *102*(D7), 8,909–8,930.

Chai, T., et al. (2007), Four-dimensional data assimilation experiments with International Consortium for Atmospheric Research on Transport and Transformation ozone measurements, *Journal of Geophysical Research*, *112*(D12S15), *doi:10.1029/2006JD007763*.

Clark, H. L., M.-L. Cathala, H. Teyssèdre, J.-P. Cammas, and V.-H. Peuch (2006), Cross-tropopause fluxes of ozone using assimilation of MOZAIC observations in a global CTM, *Tellus*, *59B*, 39–49.

Clough, S. A., et al. (2006), Forward model and jacobians for Tropospheric Emission Spectrometer retrievals, *IEEE Transactions on Geoscience and Remote Sensing*, *44*(5), 1,308–1,323.

Cooper, O. R., et al. (2006), Large upper tropospheric ozone enhancements above midlatitude north america during summed: In situ evidence from the IONS and MOZAIC ozone measurement network, *Journal of Geophysical Research*, *111*(D24S05), *doi:10.1029/2006JD007306*.

Cooper, O. R., et al. (2007), Evidence for a recurring eastern North American upper tropospheric ozone maximum during summer, *Journal of Geophysical Research*, *112*(D23304), *doi:10.1029/2007JD008710*.

Duncan, B. N., R. V. Martin, A. C. Staudt, R. Yevich, and J. A. Logan (2003), Interannual and seasonal variability of biomass burning emissions constrained by satellite observations, *Journal of Geophysical Research*, *108*(D2,4100), *doi:10.1029/2002JD002378*.

Duncan, B. N., J. A. Logan, I. Bey, I. A. Megretskaia, R. M. Yantosca, P. C. Novelli, N. B. Jones, and C. P. Rinsland (2007), Global budget of co, 1988-1997: Source estimates and validation with a global model, *Journal of Geophysical Research*, *112*(D22301), *doi:10.1029/2007JD008459*.

Elbern, H., and H. Schmidt (2001), Ozone episode analysis by four-dimensional variational chemistry data assimilation, *Journal of Geophysical Research*, *106*(D4), 3,569–3,590.

Fiore, A. M., D. J. Jacob, H. Y. Liu, R. M. Yantosca, T. D. Fairlie, and Q. Li (2003), Variability in surface ozone background over the United States: Implications for air quality policy, *Journal of Geophysical Research*, *108*(D24), *doi:10.1029/2003JD003855*.

Fishman, J., A. E. Wozniak, and J. K. Creilson (2003), Global distribution of tropospheric ozone from satellite measurements using the empirically corrected tropospheric ozone residual technique: Identification of the regional aspects of air pollution, *Atmospheric Chemistry and Physics*, *3*, 893–907.

Geer, A. J., et al. (2006), The ASSET intercomparison of ozone analyses: method and first results, *Atmospheric Chemistry and Physics*, *6*, 5,445–5,474.

GFDL GAMDT (2003), The new GFDL global atmosphere and land model AM2-LM2: Evaluation with prescribed sst simulations, *Journal of Climate*, *17*(24), 4,641–4,673.

Horowitz, L. W. (2006), Past, present and future concentrations of tropospheric ozone and aerorols: Methodology, ozone evaluation, and sensitivity to aerosol wet removal, *Journal of Geophysical Research*, *111*(D22211), *doi:10.1029/2005JD006937*.

Horowitz, L. W., et al. (2003), A global simulation of tropospheric ozone and related tracers: Description and evaluation of MOZART, version 2, *Journal of Geophysical Research*, *108*(D24), *doi:10.1029/2002JD002853*.

Hudman, R. C., et al. (2004), Ozone production in transpacific Asian pollution plumes and implications for ozone air quality in California, *Journal of Geophysical Research*, *109*(D23S10), *doi:10.1029/2004JD004974*.

Hudman, R. C., et al. (2007), Surface and lightning sources of nitrogen oxides over the United States: Magnitudes, chemical evolution and outflow, *Journal of Geophysical Research*, *112*(D12S05), *doi:10.1029/2006JD007912*.

Jones, D. B. A., K. W. Bowman, P. I. Palmer, J. R. Worden, D. J. Jacob, R. N. Hoffman, I. Bey, and R. M. Yantosca (2003), Potential of observations from the Tropospheric Emission Spectrometer to constrain continental sources of carbon monoxide, *Journal of Geophysical Research*, *108*(D24), *doi:10.1029/2003JD003702*.

Jourdain, L., et al. (2007), Tropospheric vertical distribution of tropical Atlantic ozone observed by TES during the northern African biomass burning season, *Geophysical Research Letters*, *34*(L04810), *doi:10.1029/2006GL028284*.

Khattatov, B. V., J.-F. Lamarque, L. V. Lyjak, R. Menard, P. Levelt, X. Tie, G. P. Brasseur, and J. C. Gille (2000), Assimilation of satellite observations of long-lived chemical species in global chemistry transport models, *Journal of Geophysical Research*, *105*(D23), 29,135–29,144.

Kulawik, S. S., G. Osterman, D. B. A. Jones, and K. W. Bowman (2006), Calculation of altitude-dependent Tikhonov constraints for TES nadir retrievals, *IEEE Transactions on Geoscience and Remote Sensing*, *44*(5), 1,334–1,342.

Lahoz, W. A., et al. (2007), The Assimilation of Envisat data (ASSET) project, *Atmospheric Chemistry and Physics*, *7*, 1,773–1,796.

Lamarque, J.-F., B. V. Khattatov, and J. C. Gille (2002), Constraining tropospheric ozone column through data assimilation, *Journal of Geophysical Research*, *107*(D22), *doi:10.1029/2001JD001249*.

Lawrence, M. G., et al. (2003), Global chemical weather forecasts for field campaign planning: predictions and observations of large-scale features during MINOS, CONTRACE, and INDOEX, *Atmospheric Chemistry and Physics*, *3*, 267–289.

Li, Q., D. J. Jacob, R. J. Park, Y. Wang, C. L. Heald, R. C. Hudman, R. M. Yantosca, R. V. Martin, and M. J. Evans (2005), North American pollution outflow and the trapping of convectively

lifted pollution bu upper-level anticyclone, *Journal of Geophysical Research*, *110*(D10301), *doi:10.1029/2004JD005039*.

Liang, Q., et al. (2007), Summertime influence of Asian pollution in the free troposphere over North America, *Journal of Geophysical Research*, *112*(D12S11), *doi:10.1029/2006JD007919*.

Logan, J. A. (1994), Trends in the vertical distribution of ozone: An analysis of ozonesonde data, *Journal of Geophysical Research*, *99*(D12), 25,553–25,585.

Logan, J. A. (1999), An analysis of ozonesonde data for the troposphere: Recommendations for testing 3-D models and development of a gridded climatology for tropospheric ozone, *Journal of Geophysical Research*, *104*(D13), 16,115–16,149.

Luo, M., et al. (2007a), Comparison of carbon monoxide measurements by tes and mopitt: Influence of a priori data and instrument characteristics on nadir atmospheric species retrievals, *Journal of Geophysical Research*, *112*(D09303), *doi:10.1029/2006JD007663*.

Luo, M., et al. (2007b), Tes carbon monoxide validation with dacom aircraft measurements during intex-b 2006, *Journal of Geophysical Research*, *112*(D24S48), *doi:10.1029/2007JD008803*.

McLinden, C. A., S. C. Olsen, B. Hannegan, O. Wild, and M. J. Prather (2000), Stratospheric ozone in 3-D models: A simple chemistry and the cross-tropopause flux, *Journal of Geophysical Research*, *105*(D11), 14,653–14,665.

Ménard, R., S. E. Cohn, L.-P. Chang, and P. M. Lyster (2000), Assimilation of stratospheric chemical tracer observations using a Kalman Filter. Part I: Formulation, *Monthly Weather Review*, *128*, 2,654–2,671.

Munro, R., R. Siddans, W. J. Reburn, and B. J. Kerridge (1998), Direct measurement of tropospheric ozone distributions from space, *Nature*, *392*(6672), 168–171.

Nasser, R., J. A. Logan, H. M. Worden, I. A. Megretskaia, K. W. Bowman, G. B. Osterman, A. M. Thompson, D. W. Tarasick, et al. (in press), Validation of Tropospheric Emission Spectrometer (TES) nadir ozone profiles using ozonesonde measurements, *Journal of Geophysical Research*.

Oltmans, S. J., et al. (2006), Long-term changes in tropospheric ozone, *Atmospheric Environment*, *40*, 3,156–3,173.

Osterman, G., et al. (2007), Validation of Tropospheric Emission Spectrometer (TES) measurements of the total stratospheric and tropospheric column abundance of ozone, *Journal of Geophysical Research*, *submitted*.

Pickering, K. E., Y. Wang, W. Tao, C. Price, and J.-F. Müller (1998), Vertical distributions of lightning no_x for use in regional and global chemical transport models, *Journal of Geophysical Research*, *103*(D23), 31,203–31,216.

Pierce, R. B., et al. (2007), Chemical data assimilation estimates of continental U.S. ozone and nitrogen budgets during the Intercontinental Chemical Transport Experiment-North America, *Journal of Geophysical Research*, *112*(D12S21), *doi:10.1029/2006JD007722*.

Price, C., and D. Rind (1992), A simple lightning parameterization for calculating global lightning distributions, *Journal of Geophysical Research*, *97*(D9), 9,919–9,933.

Price, C., J. Penner, and M. Prather (1997), No_x from lightning: 1. global distribution based on lightning physics, *Journal of Geophysical Research*, *102*(D5), 5,929–5,941.

Randel, W. J., and F. Wu (1999), A stratospheric ozone trends data set for global modeling studies, *Geophysical Research Letters*, *26*(20), 3,089–3,092.

Rodgers, C. D. (2000), *Inverse Methods for Atmospheric Sounding: Theory and Practice*, World Scientific.

Sauvage, B., R. V. Martin, A. van Donkelaar, X. Liu, K. Chance, L. Jaeglé, P. I. Palmer, S. Wu, and T.-M. Fu (2007), Remote sensed and *in situ* constraints on processes affecting tropical tropospheric ozone, *Atmospheric Chemistry and Physics*, *7*, 815–838.

Segers, A. J., H. J. Eskes, R. J. van der A, R. F. van Oss, and P. F. J. van Velthoven (2005), Assimilation of GOME ozone profiles and a global chemitry-transport model, using a Kalman Filter with anisotropic covariance, *Quarterly Journal of the Royal Meteorological Society*, *131*, 477–502.

Stevenson, D. S., et al. (2006), Multimodel ensemble simulations of present-day and near-future tropospheric ozone, *Journal of Geophysical Research*, *111*(D08301), *doi:10.1029/2005JD006338*.

TES Science Team (2006), TES L2 Data User's Guide, *Jet Propulsion Laboratory, California Institute of Technology*, *http://tes.jpl.nasa.gov/docsLinks/DOCUMENTS/TES Validation Report v2.0.pdf*

Tarasick, D. W., V. E. Fioletov, D. I. Wardle, J. B. Kerr, and J. Davies (2005), Changes in the vertical distribution of ozone over Canada from ozonesondes: 1980-2001, *Journal of Geophysical Research*, *110*(D02304), *doi:10.1029/2004JD04643*.

Tellmann, S., V. V. Rozanov, M. Weber, and J. P. Burrows (2004), Improvements in the tropical ozone profile retrieval from GOME-UV/Vis nadir spectra, *Advances in Space Research*, *34*(4), 739–743.

Thompson, A. M., et al. (2007a), Intercontinental Chemical Transport Experiment Ozonesonde Network Study (IONS) 2004: 1. Summertime upper troposphere/lower stratosphere ozone over northeastern North America, *Journal of Geophysical Research*, *112*(D12S12), *doi:10.1029/2006JD007441*.

Thompson, A. M., et al. (2007b), Intercontinental Chemical Transport Experiment Ozonesonde Network Study (IONS) 2004: 1. Tropospheric ozone budgets and variability over northeastern North America, *Journal of Geophysical Research*, *112*(D12S13), *doi:10.1029/2006JD007670*.

Tie, X., S. Madronich, S. Walters, D. P. Edwards, P. Ginoux, N. Mahowald, R. Y. Zhang, C. Lou, and G. P. Brasseur (2005), Assessment of the global impact of aerosols on tropospheric oxidants, *Journal of Geophysical Research*, *110*(D03204), *doi:10.1029/2004JD005359*.

Wild, O. (2007), Modelling the global tropospheric ozone budget: exploring the variability in current models, *Atmospheric Chemistry and Physics*, *7*, 2,643–2,660.

Worden, H. M., et al. (2007), Comparisons of Tropospheric Emission Spectrometer (TES) ozone profiles to ozonesondes: Methods and initial results, *Journal of Geophysical Research*, *112*(D03309), *doi:10.1029/2006JD007258*.

Yevich, R., and J. A. Logan (2003), An assessment of biofuel use and burning of agricultural waste in the developing world, *Global Biogeochemical Cycles*, *17*(4), 1095, *doi:10.1029/2002GB001952*.

Figure Captions

Figure 1. TES ozone and CO retrieval characteristics for 15 August 2006. Plots (a) and (c) show the degrees of freedom for signal (DOFS) for both the full (black crosses) and tropospheric (red crosses) ozone and CO profiles, respectively, as a function of latitude. Plots (b) and (d) show an example of an ozone and a CO retrieval, respectively, at 30° N and 87° W with averaging kernels for the lower troposphere (red), the mid-troposphere (green), and the upper troposphere/lower stratosphere (blue).

Figure 2. Monthly mean modeled ozone distribution over North America at 5 km for August 2006 without assimilation (top row) and with assimilation (middle row). The percentage differences between the assimilated and non-assimilated model runs are shown in the bottom row. The left column corresponds to the modeled fields from AM2-Chem, whereas the right column are the fields from GEOS-Chem.

Figure 3. Scatterplots of the AM2-Chem and GEOS-Chem ozone distribution at 5 km sampled over the domain shown in Figures and . The data for all days in August 2006, without assimilation and with assimilation of TES data are shown in plots (a) and (b) respectively. The comparison for data only on August 15 are shown in plots (c) and (d). The dashed line represents a linear fit of the data, while the dotted line is the $y = x$ line.

Figure 4. Daily mean modeled ozone distribution over North America at 5 km for 15 August 2006. The panels are arranged as in Figure .

Figure 5. Monthly averaged lightning NO_x emissions at 5 km over North America for August 2006 from (a) AM2-Chem and (b) GEOS-Chem. Units are molec $cm^{-3}\,s^{-1}$.

Figure 6. captionLatitude-altitude cross section, at 75° W on 15 August 2006, of (a) NO_x, (b) modeled ozone without assimilation, and (c) modeled ozone with assimilation. The top row shows the output from AM2-Chem, while the bottom row shows the fields from GEOS-Chem.

Figure 7. Longitude-altitude cross section of NO_x and ozone at 40° N on 15 August 2006. The plots are arranged as those in Figure .

Figure 8. Vertical cross section of NO_x and ozone in the GEOS-Chem model without NO_x emissions from lightning included in the simulation. Panels (a) and (b) are NO_x and ozone, respectively, as a function of latitude at 75° W. Panels (c) and (d) are NO_x and ozone, respectively, as a function of longitude at 40° N. The simulation is for 15 August 2006, the same as shown in Figures and .

Figure 9. Comparison of individual AM2-Chem and GEOS-Chem ozone profiles to ozonesonde profiles measured on 15 August 2006. In each plot, the ozonesonde profile is shown by the black line, the co-located GEOS-Chem profile by the blue line, and the AM2-Chem profiles by the blue lines. In each plot, the model profile obtained without TES assimilation is indicated by the dashed line, whereas the assimilated profiles are shown by the solid lines.

Figure 10. Comparison of mean ozone profiles over North American from the IONS-06 ozonesonde network and the AM2-Chem model (top row) and the GEOS-Chem model (bottom row). The left column shows the mean ozone profile (grey line) from the sonde data interpolated to the respective model vertical grid, the modeled mean ozone profile without assimilation (red dashed line), and the profile with assimilation (blue line). The middle column, shows the differences relative to the sonde data of the models without assimilation (red dashed line) and with assimilation (blue solid line). The right column shows the vertical distribution of the stan-

dard deviation of the interpolated ozonesonde data (black line) and the models with assimilation (blue) and without assimilation (red).

Figure 11. Monthly mean modeled CO distribution over North America at 5 km for 15 August 2006. The panels are arranged as in Figures and .

Figure 12. Monthly mean modeled ozone distribution over North America at 5 km for August 2006 with only TES CO assimilated (plots (a) and (b)). Plots (c) and (d) show the percentage differences between ozone from the CO only assimilation to the non-assimilated ozone fields shown in Figure (a) and (b).

Table 1. Ozone sounding stations used during the IONS-06 measurement campaign in August 2006, and the number of ozonesonde profiles involved in calculating the mean sonde profiles.

Station name	Latitude (° N)	Longitude (° E)	Number
Barbados	13.2	-59.5	23
Beltsville	39.0	-76.5	12
Boulder	40.0	-105.2	31
Bratts Lake	50.2	-104.7	29
Edmonton	53.6	-114.1	4
Egbert	44.2	-79.8	15
Holtville	32.8	-115.4	20
Houston	29.7	-95.4	16
Huntsville	35.3	-86.6	29
Kelowna	49.9	-119.4	27
Mexico	19.4	-98.6	10
Narragansett	41.5	-71.4	28
Paradox	43.9	-73.6	5
Ron Brown	29.7	-95.4	16
Sable	44.0	-60.0	28
Socorro	36.4	-106.9	25
Table Mountain	34.4	-117.7	31
Trinidad Head	40.8	-124.2	30
Valparaiso	41.5	-87.0	5
Wallops Island	37.9	-75.5	11
Walsingham	42.6	-80.6	10
Yarmouth	43.9	-66.1	13

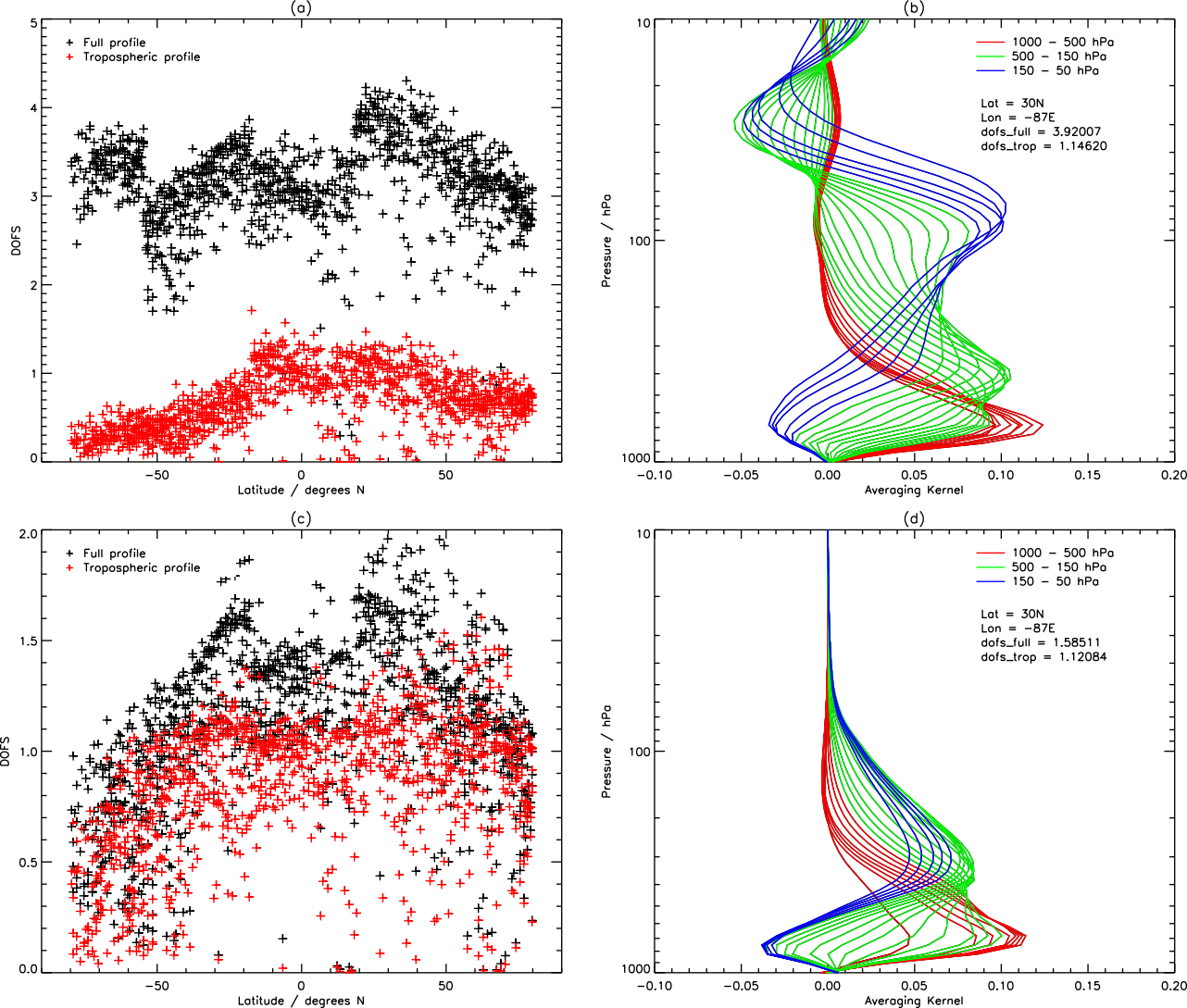
(a)
Full profile
Tropospheric profile
DOFS
Latitude / degrees N
(b)
1000 – 500 hPa
500 – 150 hPa
150 – 50 hPa
Lat = 30N
Lon = –87E
dofs_full = 3.92007
dofs_trop = 1.14620
Pressure / hPa
Averaging Kernel
(c)
Full profile
Tropospheric profile
DOFS
Latitude / degrees N
(d)
1000 – 500 hPa
500 – 150 hPa
150 – 50 hPa
Lat = 30N
Lon = –87E
dofs_full = 1.58511
dofs_trop = 1.12084
Pressure / hPa
Averaging Kernel

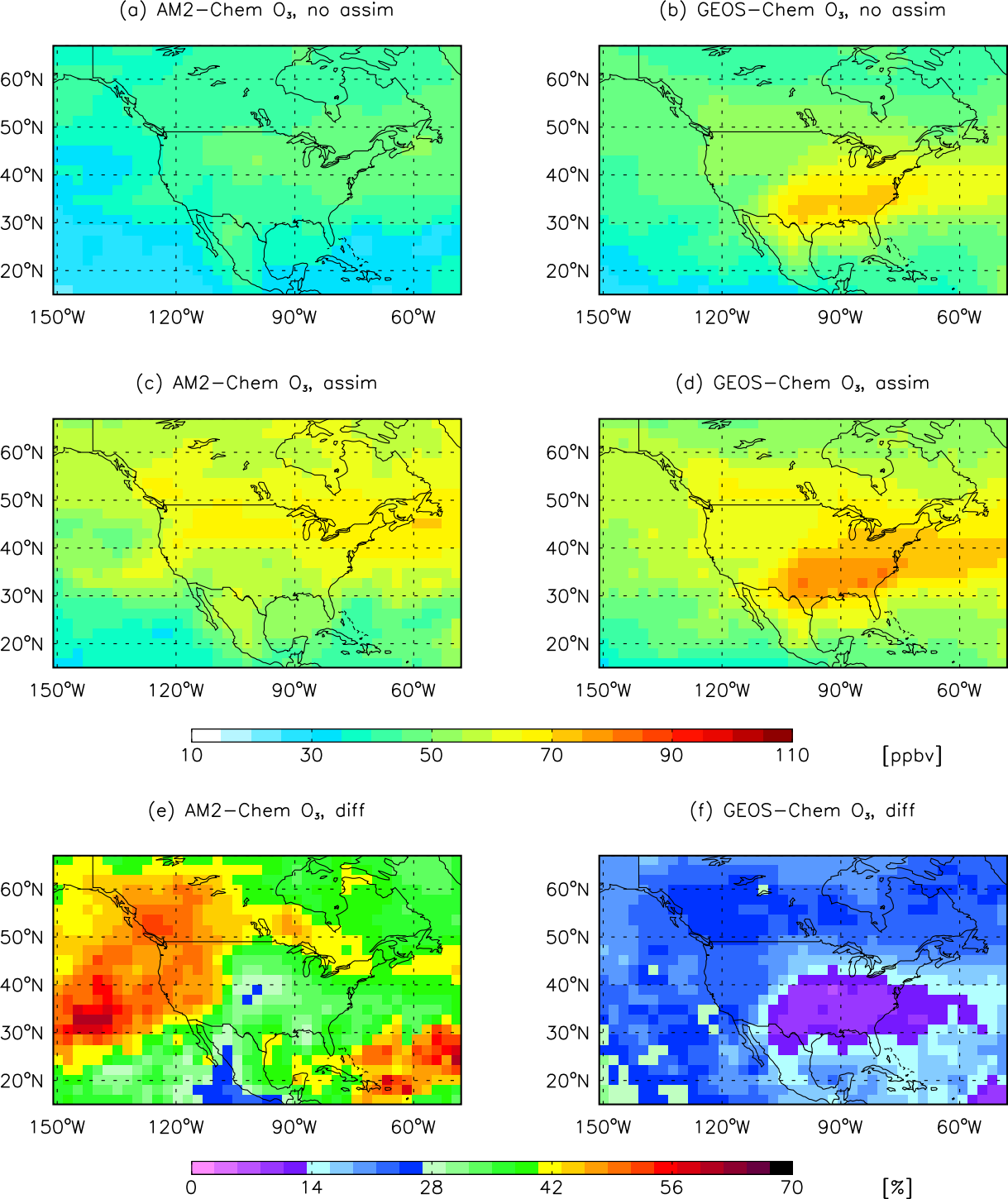
(a) AM2−Chem O₃, no assim
(b) GEOS−Chem O₃, no assim
(c) AM2−Chem O₃, assim
(d) GEOS−Chem O₃, assim
(e) AM2−Chem O₃, diff
(f) GEOS−Chem O₃, diff
60°N
50°N
40°N
30°N
20°N
150°W
120°W
90°W
60°W
10
30
50
70
90
110
[ppbv]
0
14
28
42
56
70
[%]

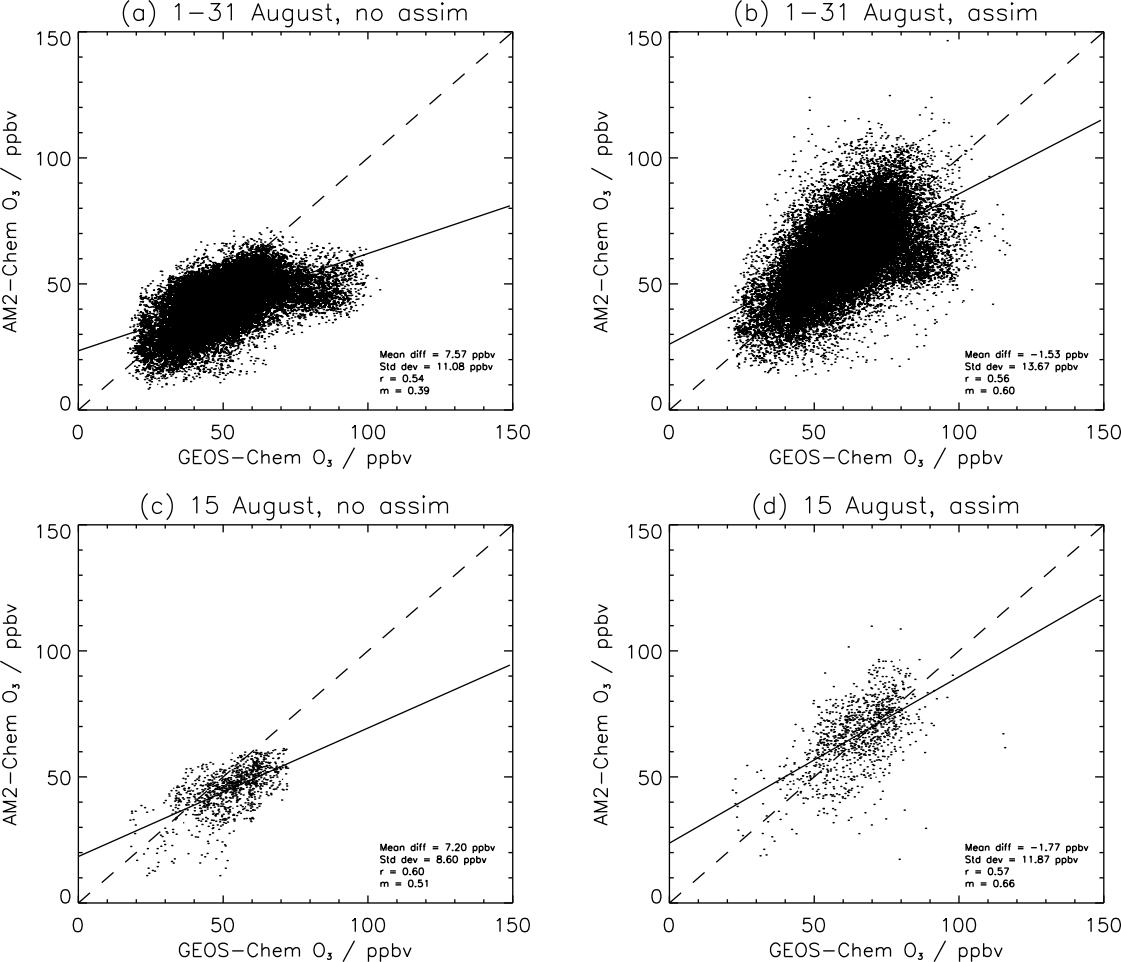
(a) 1−31 August, no assim
Mean diff = 7.57 ppbv
Std dev = 11.08 ppbv
r = 0.54
m = 0.39
(b) 1−31 August, assim
Mean diff = −1.53 ppbv
Std dev = 13.67 ppbv
r = 0.56
m = 0.60
(c) 15 August, no assim
Mean diff = 7.20 ppbv
Std dev = 8.60 ppbv
r = 0.60
m = 0.51
(d) 15 August, assim
Mean diff = −1.77 ppbv
Std dev = 11.87 ppbv
r = 0.57
m = 0.66
AM2−Chem O₃ / ppbv
GEOS−Chem O₃ / ppbv
0
50
100
150

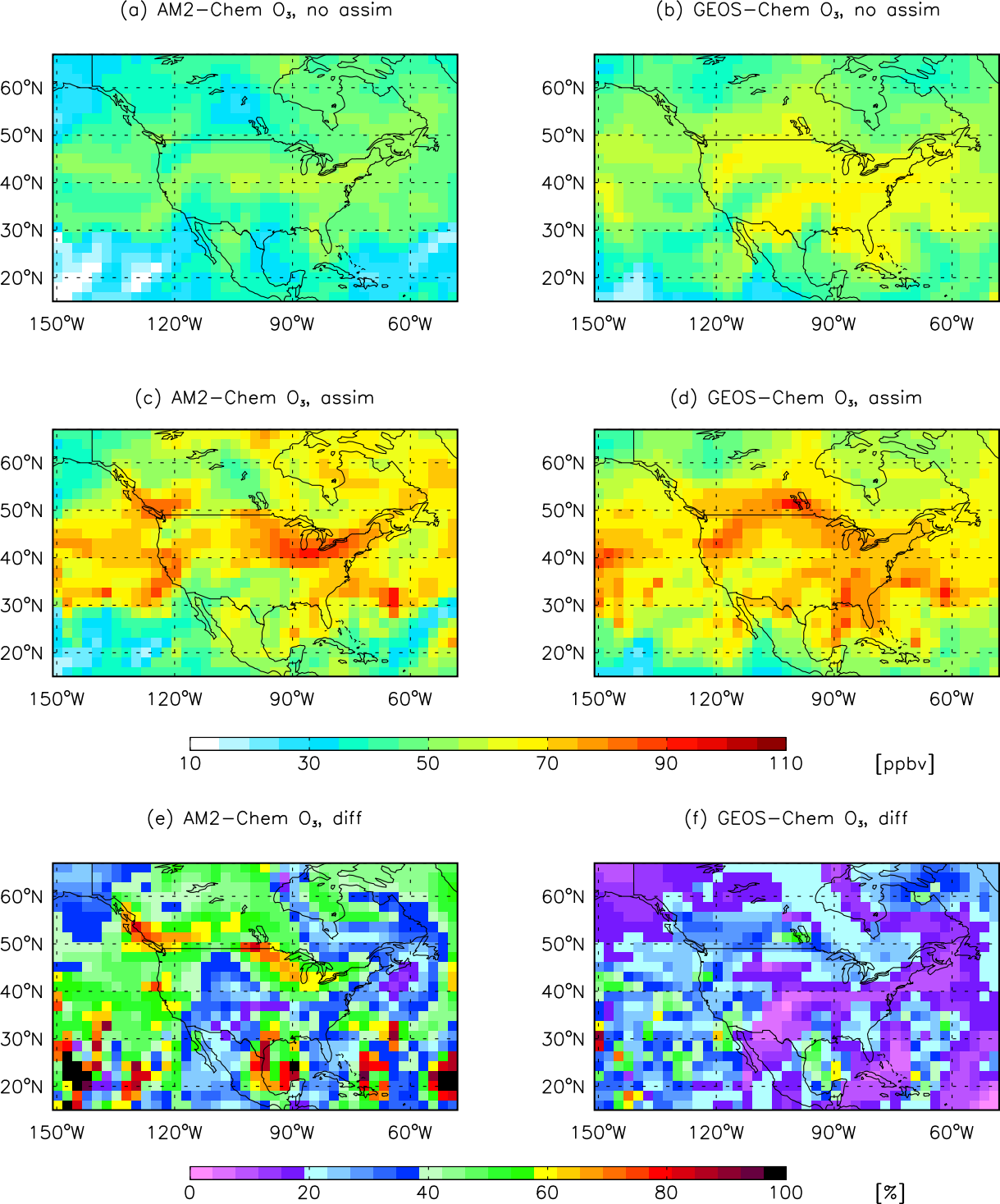
(a) AM2−Chem O₃, no assim
(b) GEOS−Chem O₃, no assim
(c) AM2−Chem O₃, assim
(d) GEOS−Chem O₃, assim
(e) AM2−Chem O₃, diff
(f) GEOS−Chem O₃, diff
60°N
50°N
40°N
30°N
20°N
150°W
120°W
90°W
60°W
10
30
50
70
90
110
[ppbv]
0
20
40
60
80
100
[%]

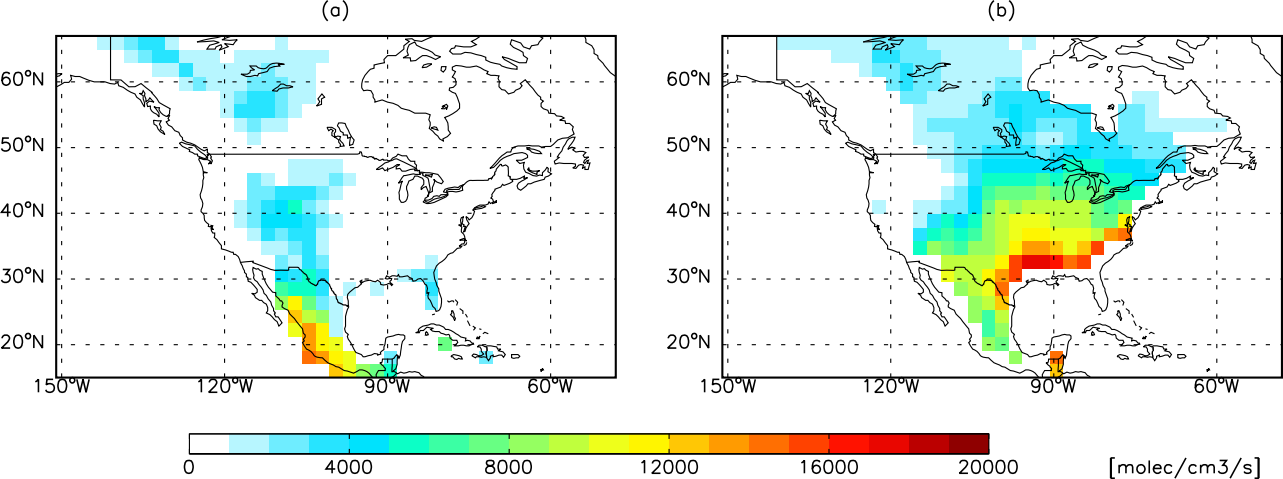
(a)
(b)
60°N
50°N
40°N
30°N
20°N
150°W
120°W
90°W
60°W
0
4000
8000
12000
16000
20000
[molec/cm3/s]

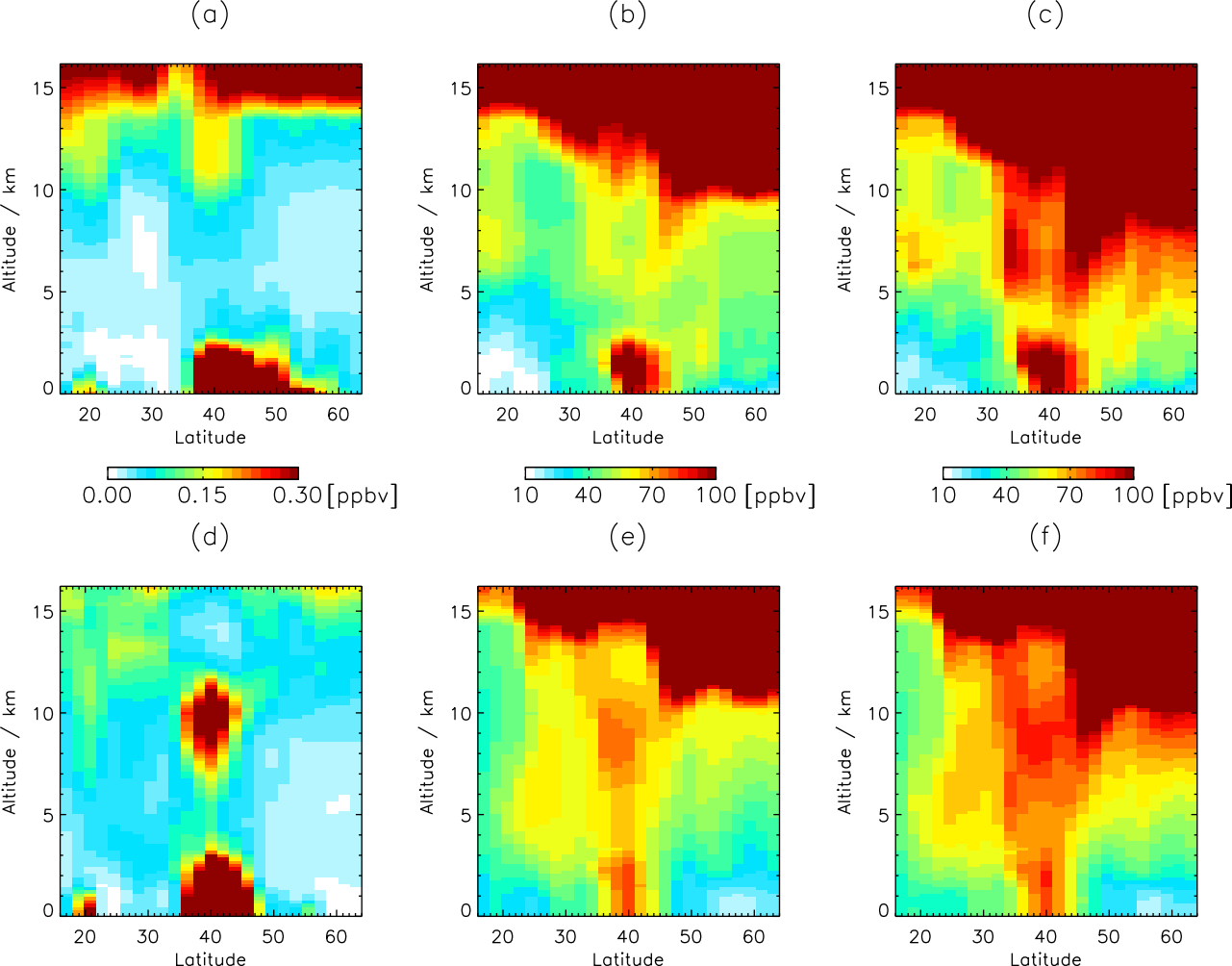
(a)
(b)
(c)
(d)
(e)
(f)
Altitude / km
Latitude
0
5
10
15
20
30
40
50
60
0.00
0.15
0.30 [ppbv]
10
40
70
100 [ppbv]

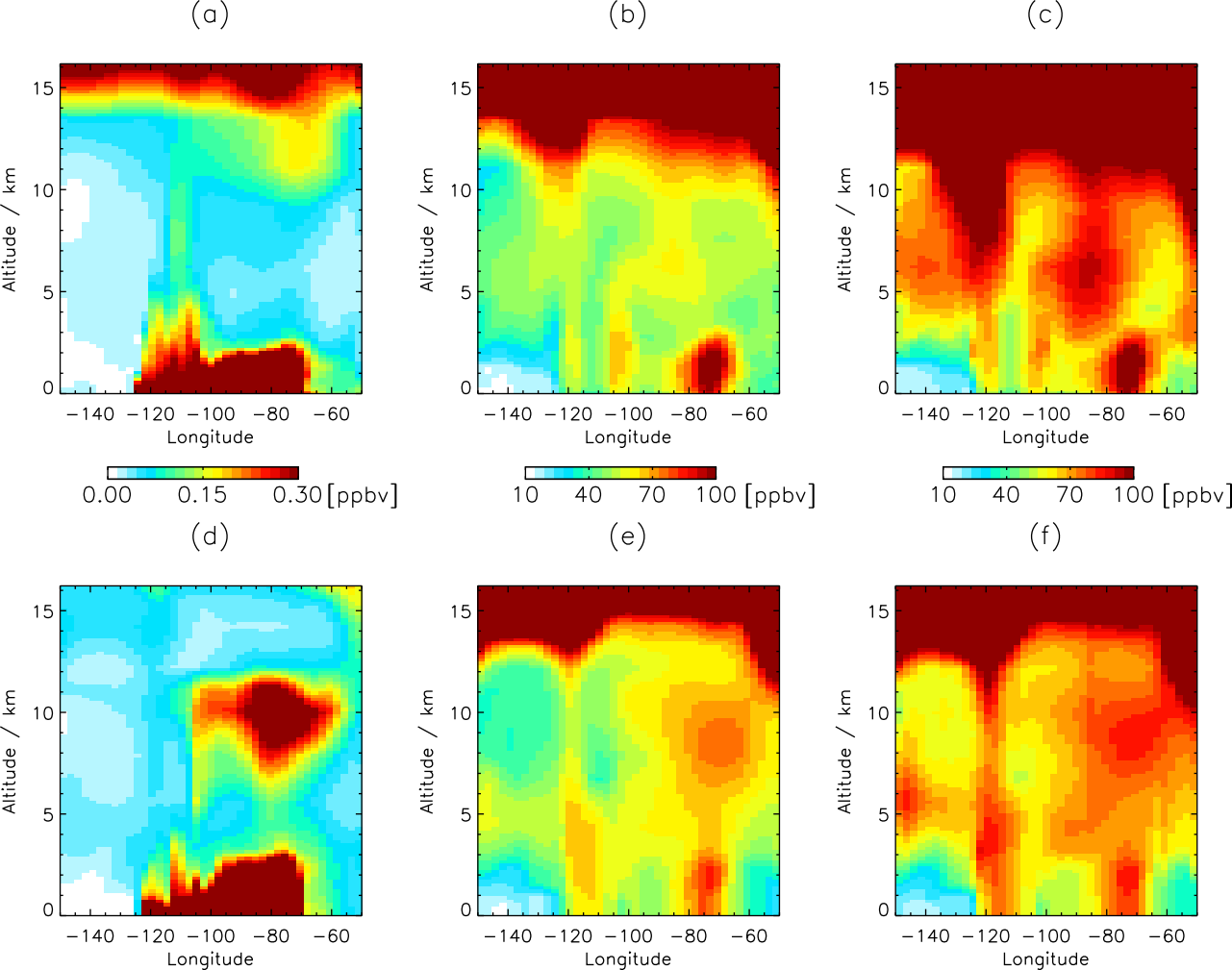
(a)
(b)
(c)
(d)
(e)
(f)
Altitude / km
Longitude
0
5
10
15
−140
−120
−100
−80
−60
0.00
0.15
0.30 [ppbv]
10
40
70
100 [ppbv]

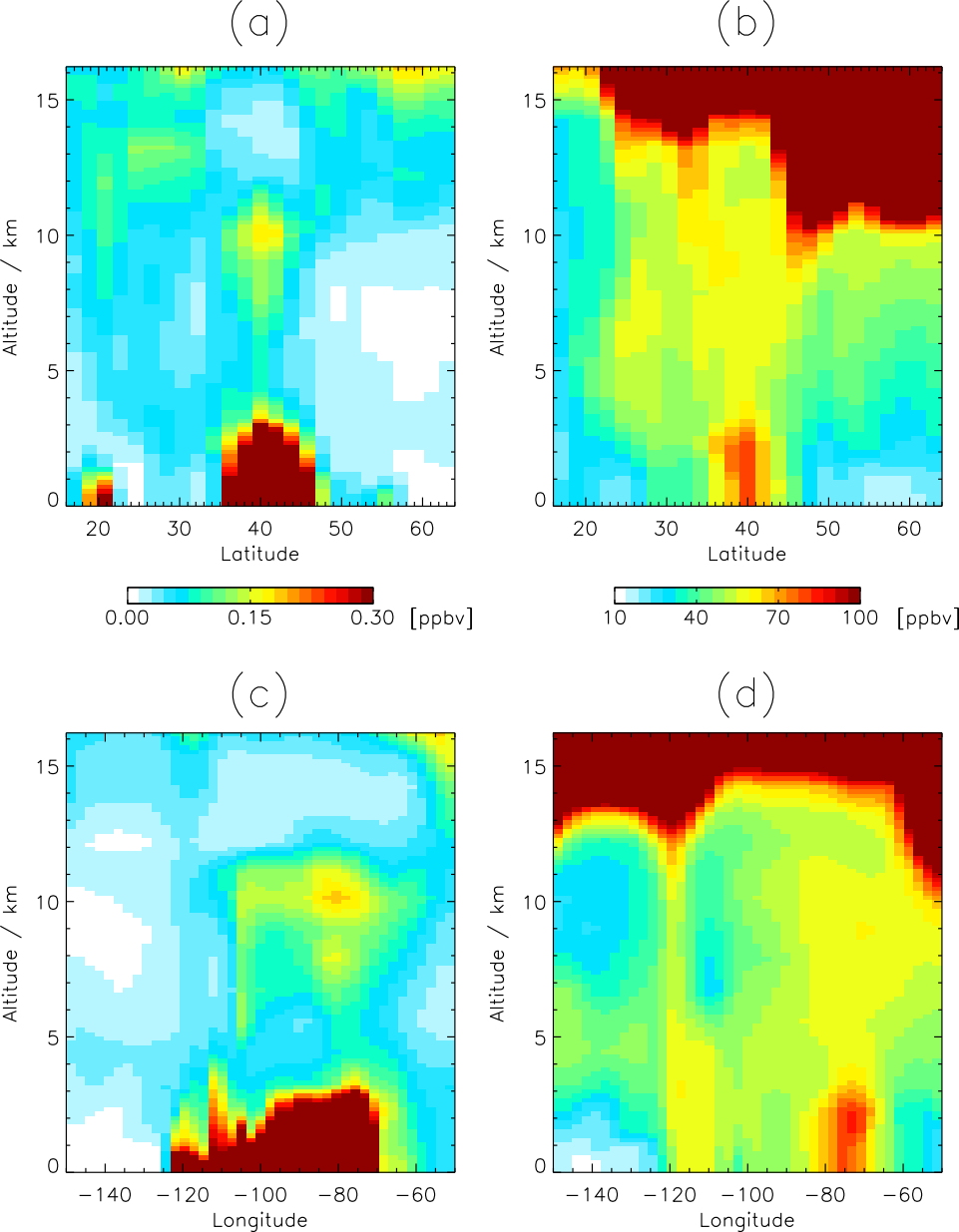
(a)
(b)
(c)
(d)
Altitude / km
Latitude
Longitude
0
5
10
15
20
30
40
50
60
−140
−120
−100
−80
−60
0.00
0.15
0.30
[ppbv]
10
40
70
100
[ppbv]

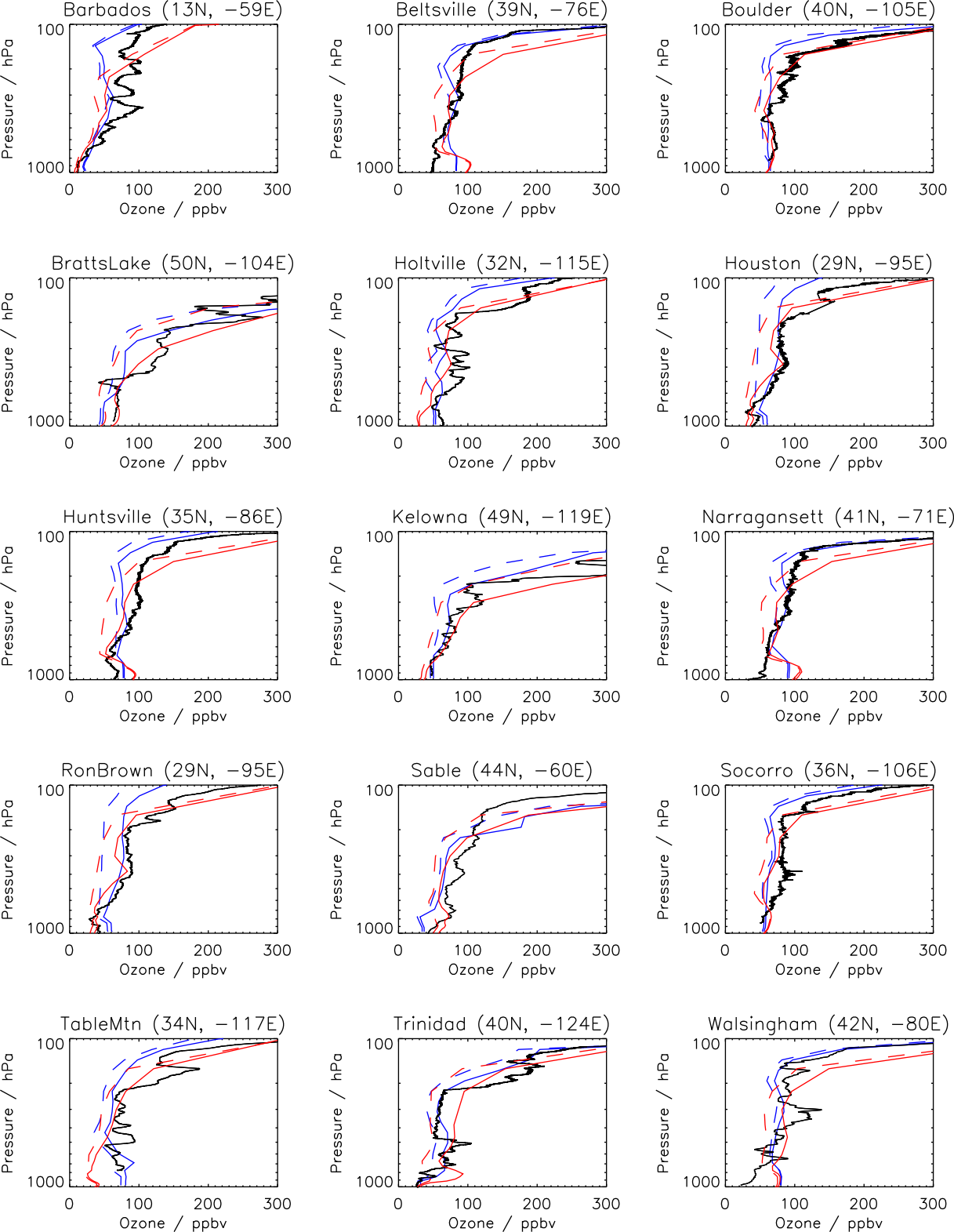
Barbados (13N, −59E)
Beltsville (39N, −76E)
Boulder (40N, −105E)
BrattsLake (50N, −104E)
Holtville (32N, −115E)
Houston (29N, −95E)
Huntsville (35N, −86E)
Kelowna (49N, −119E)
Narragansett (41N, −71E)
RonBrown (29N, −95E)
Sable (44N, −60E)
Socorro (36N, −106E)
TableMtn (34N, −117E)
Trinidad (40N, −124E)
Walsingham (42N, −80E)
Pressure / hPa
100
1000
Ozone / ppbv
0
100
200
300

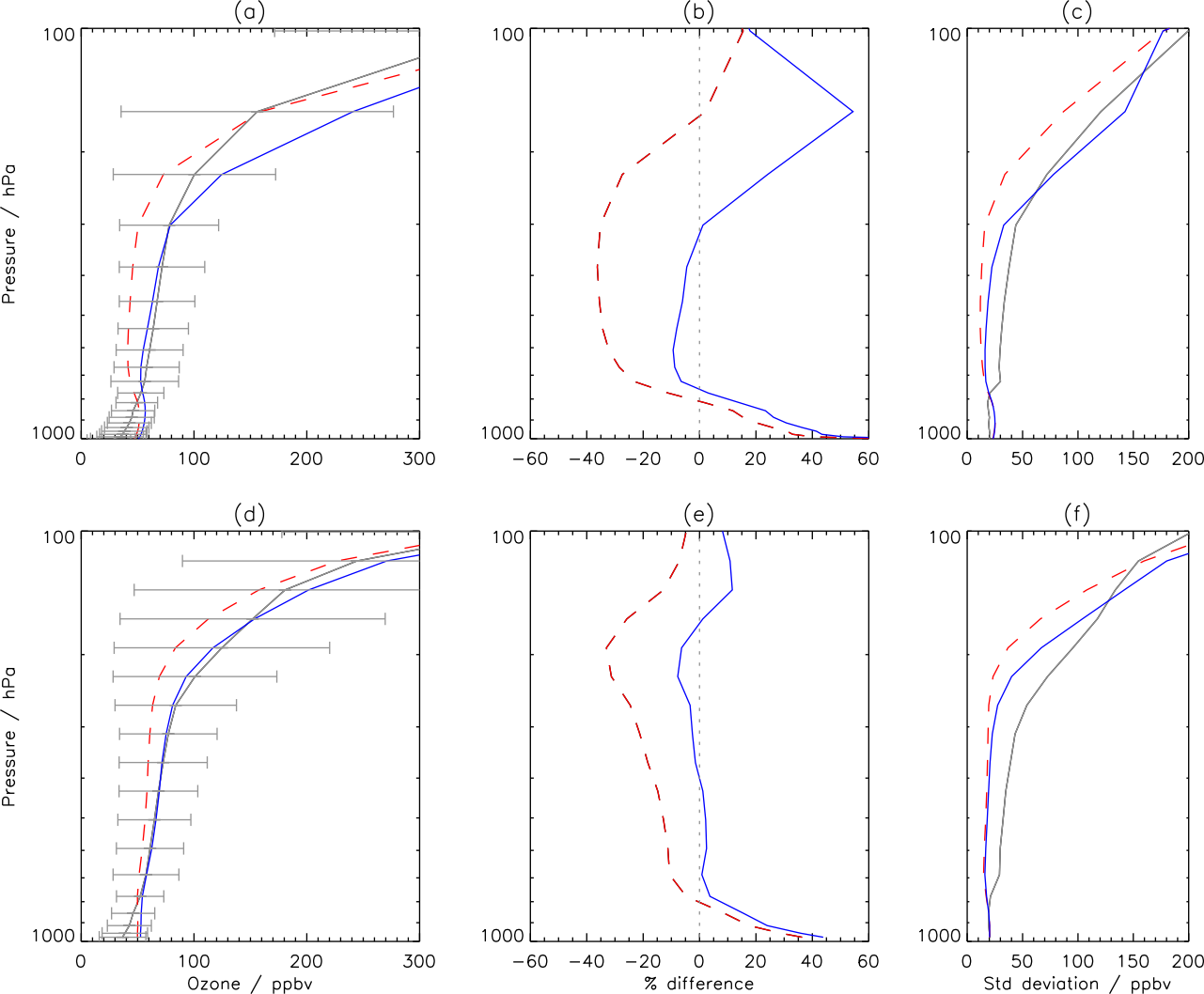
(a)
(b)
(c)
(d)
(e)
(f)
Pressure / hPa
100
1000
0
100
200
300
−60
−40
−20
0
20
40
60
50
150
Ozone / ppbv
% difference
Std deviation / ppbv

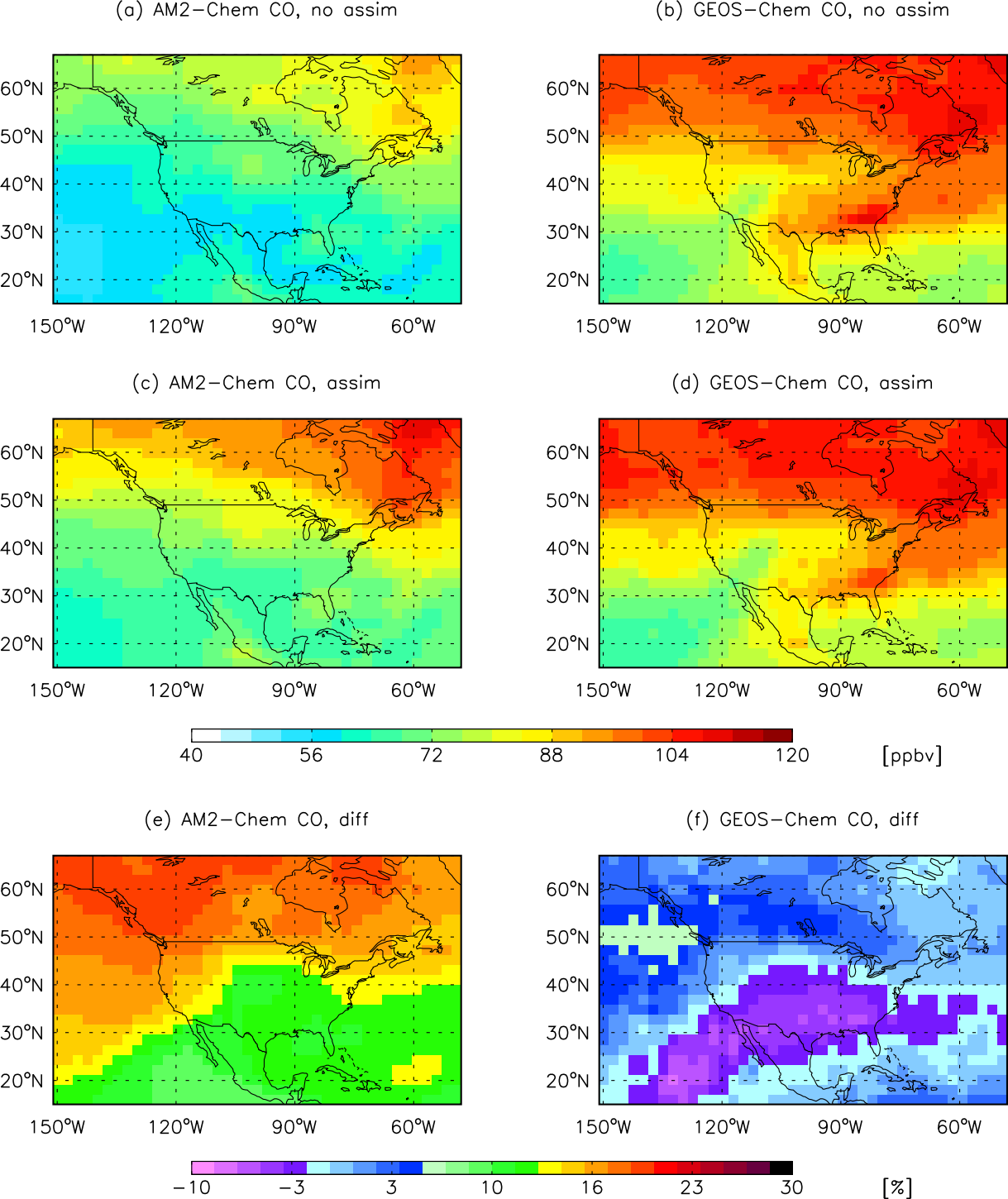
(a) AM2−Chem CO, no assim
(b) GEOS−Chem CO, no assim
(c) AM2−Chem CO, assim
(d) GEOS−Chem CO, assim
(e) AM2−Chem CO, diff
(f) GEOS−Chem CO, diff
60°N
50°N
40°N
30°N
20°N
150°W
120°W
90°W
60°W
40
56
72
88
104
120
[ppbv]
−10
−3
3
10
16
23
30
[%]

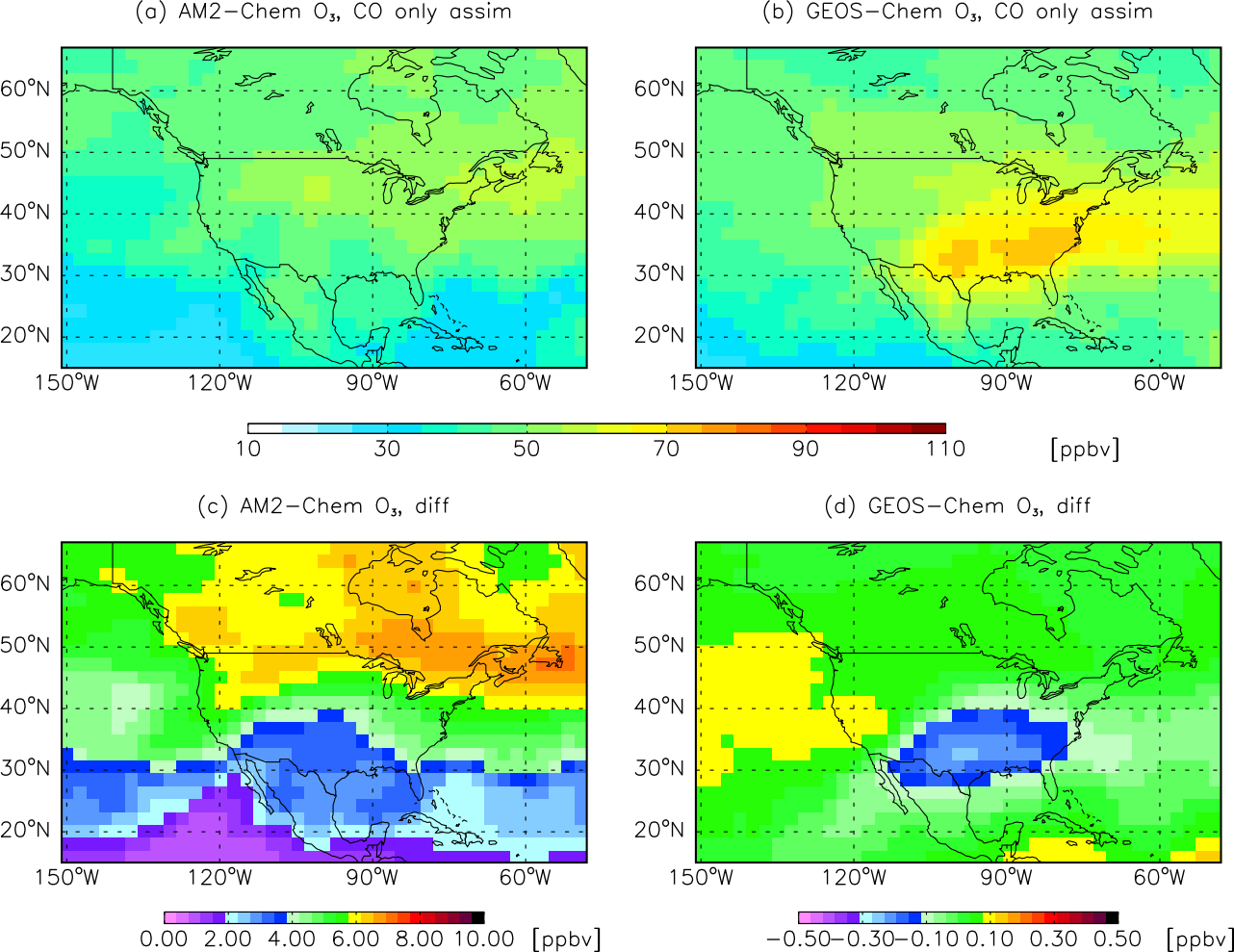
(a) AM2−Chem O₃, CO only assim
(b) GEOS−Chem O₃, CO only assim
(c) AM2−Chem O₃, diff
(d) GEOS−Chem O₃, diff
60°N
50°N
40°N
30°N
20°N
150°W
120°W
90°W
60°W
10
30
50
70
90
110
[ppbv]
0.00
2.00
4.00
6.00
8.00
10.00
[ppbv]
−0.50
−0.30
−0.10
0.10
0.30
0.50
[ppbv]